

AD-A036 332

DAVID W TAYLOR NAVAL SHIP RESEARCH AND DEVELOPMENT CE--ETC F/G 13/10  
SEAKEEPING CHARACTERISTICS OF THE XR-5, A HIGH LENGTH-BEAM RATIO--ETC(U)  
MAY 76 J J RICCI, A H MAGNUSON

UNCLASSIFIED

SPD-616-03

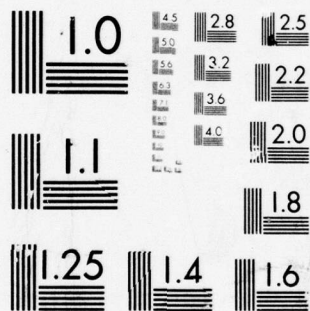
NL

| OF |  
AD  
A036332



END

DATE  
FILMED  
3-77



MICROCOPY RESOLUTION TEST CHART  
NATIONAL BUREAU OF STANDARDS-1963-A

SPD 616-03

A SEAKEEPING CHARACTERISTICS OF THE XR-5, A HIGH LENGTH-BEAM RATIO MANNED  
SURFACE EFFECT TESTCRAFT: III. RESULTS OF RANDOM WAVE EXPERIMENTS, INVESTIGATION  
OF LINEAR SUPERPOSITION FOR SHIP MOTIONS AND TRIM AND DRAFT IN RANDOM WAVES

AD A 036332

**DAVID W. TAYLOR NAVAL SHIP  
RESEARCH AND DEVELOPMENT CENTER**

Bethesda, Md. 20084



SEAKEEPING CHARACTERISTICS OF THE XR-5, A HIGH  
LENGTH-BEAM RATIO MANNED SURFACE EFFECT TESTCRAFT:  
III. RESULTS OF RANDOM WAVE EXPERIMENTS, INVESTIGATION  
OF LINEAR SUPERPOSITION FOR SHIP MOTIONS AND TRIM AND  
DRAFT IN RANDOM WAVES

by

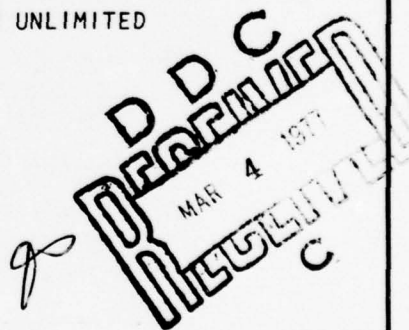
Joseph J. Ricci  
and  
Allen H. Magnuson.

APPROVED FOR PUBLIC RELEASE: DISTRIBUTION UNLIMITED

SHIP PERFORMANCE DEPARTMENT

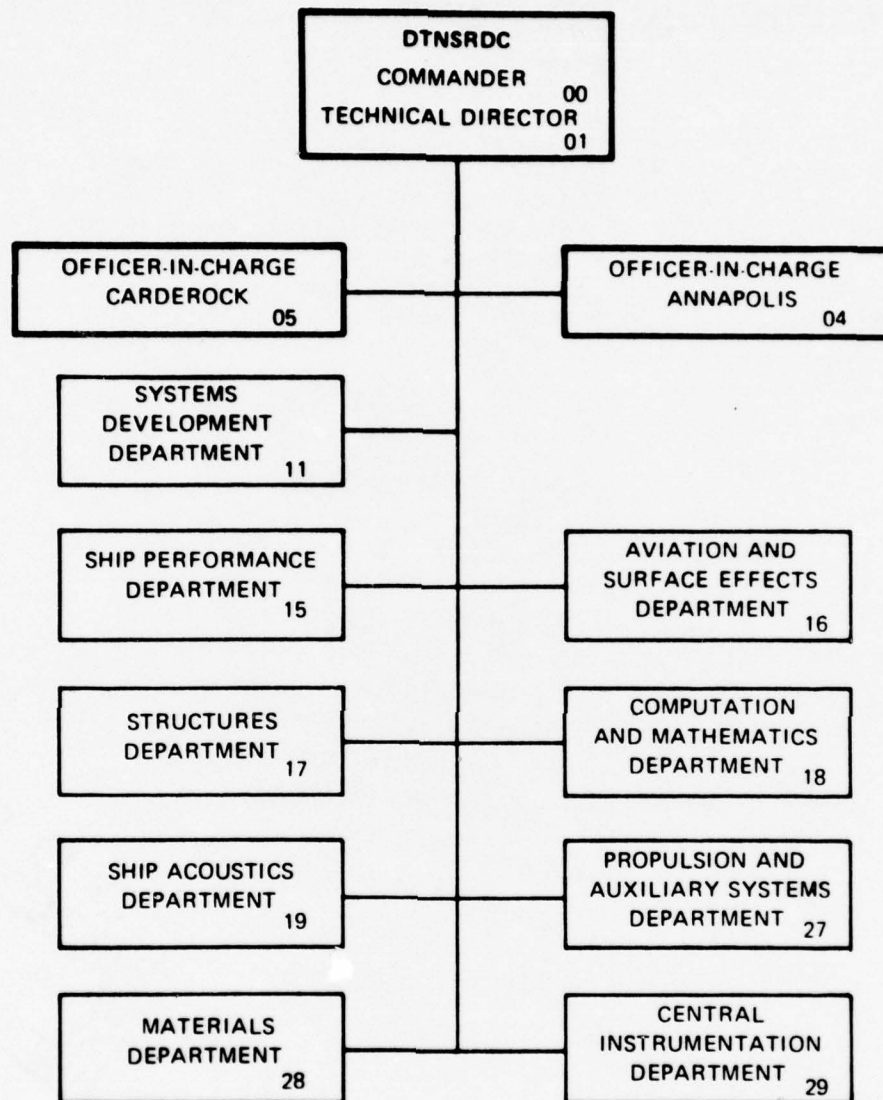
MAY 1976

SPD 616-03



ENCLOSURE (1)

## MAJOR DTNSRDC ORGANIZATIONAL COMPONENTS





UNCLASSIFIED

SECURITY CLASSIFICATION OF THIS PAGE (When Data Entered)

REPORT DOCUMENTATION PAGE		READ INSTRUCTIONS BEFORE COMPLETING FORM
1. REPORT NUMBER SPD-616-03	2. GOVT ACCESSION NO.	3. RECIPIENT'S CATALOG NUMBER
4. TITLE (and Subtitle) Seakeeping Characteristics of the XR-5, A High Length-Beam Ratio Manned Surface Effect Testcraft: III. Results of Random Wave Experiments. Investigation of Linear Superposition for Ship Motions and Trim and Draft in Random Waves		5. TYPE OF REPORT & PERIOD COVERED
7. AUTHOR(s) Joseph J./Ricci and Allen H./Magnuson		6. PERFORMING ORG. REPORT NUMBER
9. PERFORMING ORGANIZATION NAME AND ADDRESS David W. Taylor Naval Ship Research and Development Center, Ship Performance Department Bethesda, Maryland 20084		8. CONTRACT OR GRANT NUMBER(s) F43421 SF 43421202
11. CONTROLLING OFFICE NAME AND ADDRESS		10. PROGRAM ELEMENT, PROJECT, TASK AREA & WORK UNIT NUMBERS Task Area SF 43421202 Work Unit Number 1-1507-200
14. MONITORING AGENCY NAME & ADDRESS (if different from Controlling Office)		12. REPORT DATE May 1976
		13. NUMBER OF PAGES 62
		15. SECURITY CLASS. (of this report) UNCLASSIFIED
		15a. DECLASSIFICATION/DOWNGRADING SCHEDULE
16. DISTRIBUTION STATEMENT (of this Report)  APPROVED FOR PUBLIC RELEASE: DISTRIBUTION UNLIMITED		
17. DISTRIBUTION STATEMENT (of the abstract entered in Block 20, if different from Report)		
18. SUPPLEMENTARY NOTES		
19. KEY WORDS (Continue on reverse side if necessary and identify by block number)  Seakeeping; Irregular Waves; High Length-Beam Ratio Surface Effect Ship		
20. ABSTRACT (Continue on reverse side if necessary and identify by block number) Motion responses derived from model experimental results in regular and irregular head waves for the XR-5 high length-beam ratio surface effect ship are presented. Frequency response functions for pitch, heave, relative bow motion, heave acceleration and bow acceleration were computed from the random wave experiments and are presented herein. Comparisons are made with responses derived from regular wave experiments. The results indicate that the rigid body motions are reasonably linear for the Froude numbers and sea conditions investigated. Nonlinear effects that increase with the severity of the sea		

DD FORM 1 JAN 73 1473

EDITION OF 1 NOV 65 IS OBSOLETE  
S/N 0102-014-6601

UNCLASSIFIED

SECURITY CLASSIFICATION OF THIS PAGE (When Data Entered)

389694

bpg

UNCLASSIFIED

SECURITY CLASSIFICATION OF THIS PAGE(When Data Entered)

state are evident in the accelerations.

In addition, the motion of the stern seal with respect to the relative motion at the stern is presented. These responses are generally linear although some nonlinear effects appear with increasing Froude number.

Probability distributions for the double amplitude of wave height, heave and pitch are presented. Comparisons are made with Rayleigh probability distributions based on the variances of the sample data and on the minimum Chi Square <sup>(2)</sup> estimators computed from the distributions.

APPROVED FOR	
RUC	White Section
DDC	Buff Section
UNCLASSIFIED	
JUSTIFICATION	
BY	
DISTRIBUTION/AVAILABILITY	
DATE	
A	

UNCLASSIFIED

SECURITY CLASSIFICATION OF THIS PAGE(When Data Entered)

## TABLE OF CONTENTS

	Page
ABSTRACT	1
ADMINISTRATIVE INFORMATION	1
INTRODUCTION	2
DESCRIPTION OF MODEL	2
EXPERIMENTAL SETUP	3
EXPERIMENTAL PROCEDURE	4
DATA ANALYSIS	5
PRESENTATION OF DATA	6
DISCUSSION OF RESULTS	8
SUMMARY AND CONCLUSIONS	12
ACKNOWLEDGMENTS	13
REFERENCES	14

## LIST OF TABLES

	Page
Table 1 - XR-5 Model Characteristics	15
Table 2 - Transducer Locations	16
Table 3 - Operating Conditions for Model	17
Table 4 - Speeds in Knots for Various Scale Ratios of XR-5 High L/B SES, As a Function of Froude Number	18
Table 5 - Summary of Random Wave Conditions	19
Table 6 - Significant Double Amplitude Motions	20
Table 7 - Significant Double Amplitude Accelerations	21

# LIST OF FIGURES

	Page
Figure 1 - Side View of Model and Towing Gear with Model Clear of Water	22
Figure 2 - The XR-5 Manned Testcraft	23
Figure 3 - XR-5 Model in Random Waves; $F_n = 0.96$ , Sig. W.H./Cushion Depth = .309	24
Figure 4 - XR-5 Model in Random Waves; $F_n = 0.96$ , Sig. W.H./Cushion Depth = .693	25
Figure 5 - Mean Draft Per Unit Cushion Depth Versus Normalized Significant Waveheight ( $F_n = 0.72 - 1.20$ )	26
Figure 6 - Ratio of Accelerations Computed from Linear Superposition to Those Computed from Double Amplitude Distributions Versus Normalized Waveheight ( $F_n = 0.72 - 0.96$ )	27
Figure 7 - Encounter Wave Spectra at 9 Knots, $F_n = 0.72$	28
Figure 8 - Encounter Wave Spectra at 12 Knots, $F_n = 0.96$	29
Figure 9 - Encounter Wave Spectra at 15 Knots, $F_n = 1.20$	30
Figure 10 - Comparison of Basin-Generated Wave Spectrum with a one-parameter Pierson Moskowitz Spectral Representation for the same Significant Wave Height	31
Figure 11 - Pitch Angle per Unit Wave Slope as a Function of Encounter Frequency, $F_n = 0.72$	32
Figure 12 - Pitch Angle per Unit Wave Slope as a Function of Encounter Frequency, $F_n = 0.96$	33
Figure 13 - Pitch Angle per Unit Wave Slope as a Function of Encounter Frequency, $F_n = 1.20$	34
Figure 14 - Heave Motion per Unit Wave Height as a Function of Encounter Frequency, $F_n = 0.72$	35
Figure 15 - Heave Motion per Unit Wave Height as a Function of Encounter Frequency, $F_n = 0.96$	36
Figure 16 - Heave Motion per Unit Wave Height as a Function of Encounter Frequency, $F_n = 1.20$	37



# LIST OF FIGURES (Cont'd)

	Page
Figure 17 - Relative Bow Motion per Unit Wave Height as a Function of Encounter Frequency, $F_n = 0.72$	38
Figure 18 - Relative Bow Motion per Unit Wave Height as a Function of Encounter Frequency, $F_n = 0.96$	39
Figure 19 - Relative Bow Motion per Unit Wave Height as a Function of Encounter Frequency, $F_n = 1.20$	40
Figure 20 - Bow Acceleration per Unit Wave Height as a Function of Encounter Frequency, $F_n = 0.72$	41
Figure 21 - Bow Acceleration per Unit Wave Height as a Function of Encounter Frequency, $F_n = 0.96$	42
Figure 22 - Bow Acceleration per Unit Wave Height as a Function of Encounter Frequency, $F_n = 1.20$	43
Figure 23 - Heave Acceleration per Unit Wave Height as a Function of Encounter Frequency, $F_n = 0.72$	44
Figure 24 - Heave Acceleration per Unit Wave Height as a Function of Encounter Frequency, $F_n = 0.96$	45
Figure 25 - Heave Acceleration per Unit Wave Height as a Function of Encounter Frequency, $F_n = 1.20$	46
Figure 26 - Stern Seal Motion per Unit Relative Stern Displacement as a Function of Encounter Frequency, $F_n = 0.72$	47
Figure 27 - Stern Seal Motion per Unit Relative Stern Displacement as a Function of Encounter Frequency, $F_n = 0.96$	48
Figure 28 - Stern Seal Motion per Unit Relative Stern Displacement as a Function of Encounter Frequency, $F_n = 1.20$	49
Figure 29 - Double Amplitude Distribution for Heave and Pitch, $F_n = 0.72$	50
Figure 30 - Double Amplitude Distribution for Heave and Pitch, $F_n = 0.72$	51
Figure 31 - Double Amplitude Distribution for Heave and Pitch, $F_n = 0.96$	52
Figure 32 - Double Amplitude Distribution for Heave and Pitch, $F_n = 0.96$	53

LIST OF FIGURES (Cont'd)

	Page
Figure 33 - Double Amplitude Distributions for Heave and Pitch, $F_n = 1.20$	54
Figure 34 - Experimental Transfer Functions for a Destroyer in Head Seas at 20 Knots (Full Scale Speed)	55



## ABSTRACT

Motion responses derived from model experimental results in regular and irregular head waves for the XR-5 high length-beam ratio surface effect ship are presented. Frequency response functions for pitch, heave, relative bow motion, heave acceleration and bow acceleration were computed from the random wave experiments and are presented herein. Comparisons are made with responses derived from regular wave experiments. The results indicate that the rigid body motions are reasonably linear for the Froude numbers and sea conditions investigated. Nonlinear effects that increase with the severity of the sea state are evident in the accelerations.

In addition, the motion of the stern seal with respect to the relative motion at the stern is presented. These responses are generally linear although some nonlinear effects appear with increasing Froude number.

Probability distributions for the double amplitudes of wave height, heave and pitch are presented. Comparisons are made with Rayleigh probability distributions based on the variances of the sample data and on the minimum Chi Square ( $\chi^2$ ) estimators computed from the distributions.

## ADMINISTRATIVE INFORMATION

This work was supported by the Naval Sea Systems Command and was authorized under Task Area Number SF 43421202. Work Unit Number 1-1507-200 was used. The objective of the task was to develop a capability for predicting the dynamic performance characteristics of surface effect ships for use in design evaluation. The experimental program described in this report represents the second stage of the task in which the XR-5 craft response in waves is analyzed using model experimental data.

## INTRODUCTION

The purpose of this series of seakeeping experiments was to investigate the applicability of the linear superposition assumption to determine irregular sea responses of the XR-5 craft as computed from regular wave data. The model used is a 1/3 scale replica of the XR-5 manned testcraft. Both the model and manned testcraft were built to obtain data for performance prediction of a proposed high length-beam ratio surface effect ship (SES) with an overall length of about 500 feet. The high length-beam ratio SES is designed to operate at subhump speeds. The nominal design Froude number of 0.7 is low relative to other SES and amphibious hovercraft which may have design Froude numbers of 1.5 to 2.0 or higher. This report presents the results of the irregular sea experiments for the XR-5 model in head waves at three Froude numbers. Frequency response functions obtained for regular head waves were presented in References 1 and 2.\*

## DESCRIPTION OF MODEL

A photograph of the model and tow gear is given in Figure 1. The XR-5 Manned Testcraft is shown in Figure 2. Model dimensions and transducer locations are given in Tables 1 and 2, respectively.

The model is constructed of polyurethane foam reinforced with an outer covering of fiberglass. The two sidewalls have a 45 degree deadrise except in the vicinity of the bow, where the deadrise angle is higher (see Figure 2). The bow and stern seals are the semi-rigid three-lobed planing type, and are inflated directly from stacked axial flow fans. The seal air is vented to the air cushion (main plenum) through clear plexiglass bypass ducts mounted on the deck at the bow and stern. Each duct has two adjustable gate valves that regulate the back pressure in the seal. The after valve controls the third (upper) lobe, which is designed to alleviate impact pressures. The forward or main valve regulates the two larger lobes, and thus governs the seal overpressure relative to the cushion pressure.

The model was fitted with 12 fans. Four feed the seals, and the remainder feed the main plenum directly. The fans are synchronous and

---

\* References are listed on page 14.

were run at 20,000 RPM. The fans feeding the seals were stacked, two in series, so that an overpressure relative to the main plenum would be developed. Each fan was fitted with a spring-loaded flapper, or check valve, so that no air would leak out if the fan was not working or was not switched on. The various pressures (seal and plenum) could be adjusted by selecting the number of feed fans and by means of the four gate valves in the seal bypass ducts.

The maximum downward position of each seal is limited by two sets of downstops which are short lengths of aircraft cable attached at the deck and on the seal stiffeners. The forward set of downstops is about midway between the hinge line and the trailing edge, while the after set is near the trailing edge. The maximum downstop position and the chamber of the seals could be adjusted by means of shims of various thickness which were inserted between the downstops and the deck.

#### EXPERIMENTAL SETUP

A side view of the model mounted on the towing apparatus is given in Figure 1. The towing frame is attached to the rear (East side) of Carriage II by means of an A-frame device. The pitch-heave towing gear from the Center's Tank at Langley Field, Virginia was mounted below the frame. The tow point was located forward of the model's longitudinal center of gravity (LCG) to ensure yaw stability. The tow cable was led through a sheave mounted to the heave staff to simulate a thrust axis along the lower edge of the keel. The model was free to pitch and heave. The model was fixed in surge by the tow cable, which was kept taut by applying a constant 20 pound force to the back of the surge roller cage using a force negator. Some surge motion (about one inch) occurs when the model pitches due to the tow cable's being led through the sheave on the heave staff.

The model was fitted with lifting cables forward and aft that were led to winches on the carriage so that the model could be lifted clear of the water at the end of each run to avoid swamping and to save time when returning to the other end of the basin. In addition, snubber lines were attached to the model to restrict motion in case of emergency.



The model was extensively fitted with transducers to measure motions, accelerations, pressures, and relative wave heights. The pitch-heave towing gear was equipped with slide-wire devices for measuring the heave staff position and the craft pitch angle. The heave staff and heave transducer were mounted forward of the LCG. Accelerometers were mounted at the LCG and at the bow.

Pressure transducers were mounted at the bow and stern to measure bow and stern seal pressure, and two additional pressure transducers were either flush-mounted in the plenum or had a short length of tubing leading to the high pressure side. The reference pressure was obtained by venting the low pressure side to the atmosphere in an air chamber shielded from the air stream to eliminate picking up any dynamic pressure. The transducers selected had high frequency response characteristics so that true dynamic measurements were obtained throughout the frequency range of interest. Ultrasonic wave height transducers were mounted in or on the craft at five locations: the bow, three locations in the main plenum, and the stern. The bow and stern transducers are shown in Figures 2 and 4 of Reference 1. In addition, a wave height transducer was mounted on the carriage well forward of the model to obtain a reference wave height undisturbed by the presence of the model.

#### EXPERIMENTAL PROCEDURE

Before starting the random wave program, it was necessary to establish a representative operating condition for the craft. In particular, a near-optimum fan configuration, duct valve settings and downstop settings had to be determined. This was partly done on the basis of earlier experimental data and from a series of exploratory random wave experiments in which the above parameters were adjusted to minimize motion. The duct valve settings for the reference model operating condition for the craft, are given in Table 3. The reference fan arrangement was 2-0-2, i.e., two fans in the forward seal, none in the main plenum and two in the stern seal. The downstops were set in the maximum downward position. This operating condition is not necessarily the optimum one for the craft. It was impossible to explore all the combinations of operating conditions due to

the time limitations; however, the reference condition is near-optimum from the seakeeping or ship motions standpoint, while maintaining good drag and lift fan power characteristics. The reference condition is very close to the one selected in an earlier series of experiments where the effective horsepower (fan plus propulsion) was minimized.

The irregular seas experiment was designed to examine the worst case behavior of the model in random waves by selecting encounter spectra that contained most of their energy in the same range as the resonant frequency of the model. The experiments were carried out with the model on-cushion at 9, 12 and 15 knots, corresponding to Froude numbers of 0.72 (design speed), 0.96 and 1.20. (See Table 4). At 9 and 12 knots, runs were made in two sea states with similar frequency content but different significant wave heights. A complete description of the procedure used to obtain the regular wave data is presented in References 1 and 2.

#### DATA ANALYSIS

The irregular sea data was recorded on magnetic tape and processed using a spectral analysis computer program. Data obtained in random waves were analyzed in both the time domain and the frequency domain. This analysis yields mean values, power spectra, histograms and Fourier transforms as well as statistical information about the time histories.

The heave and pitch data derived from data collected at the pitch-heave staff were combined in the time domain to determine heave at the LCG. Pitch was nondimensionalized by wave slope while stern seal motion was normalized by the relative motion at the stern. All other measurements were normalized by the wave amplitude.

Probability distributions for the double amplitude values of wave height, heave and pitch were calculated from the histograms produced by the irregular seas data analysis program. Corresponding Rayleigh distributions were computed for comparison purposes. Two Rayleigh distributions are presented; one which is based on the sample variance and one which is based on the minimum Chi-square ( $\chi^2$ ) estimator derived from the histograms.

## PRESENTATION OF DATA

Table 5 presents the mean values of trim, draft and cushion pressure obtained for five irregular wave conditions. The values in Table 5 are plotted in Figure 5 to indicate the effect of increasing sea state on the mean operating conditions of the craft. The significant wave height and mean draft are normalized by dividing by the cushion height. The mean cushion pressures are normalized by multiplying by the nominal cushion area and dividing by the craft weight.

Tables 6 and 7 present significant response, i.e. average of the one-third highest double amplitudes, determined directly from the double amplitude distributions, derived from spectra using the narrowband assumption and derived using linear superposition of the regular wave transfer functions and the measured wave spectra. Table 6 presents these results for heave, pitch and relative bow motion (RBM). Heave and RBM are normalized by the cushion height while pitch is normalized by the significant wave height to cushion height ratio. Table 7 presents similar results for absolute vertical acceleration at the bow and at the center of gravity. The acceleration has been normalized by the significant wave height to cushion height ratio.

Figures 7 through 10 are graphs of the wave spectra encountered by the model during the experiments. These would range from Sea State 4 to Sea State 6 for a 500-ft ship. These particular wave spectra were chosen because their significant energy content corresponded to the model's natural frequency of 6 radians per second. Figure 10 is included to demonstrate the difference between the experimental spectra chosen for these experiments and the one-parameter (significant wave height) Pierson-Moskowitz (PM) spectrum.

One sees from Figures 7, 8 and 9 that the peaks of the spectra coincide closely with the model's natural frequency. Two spectra are shown in Figures 7 and 8 (for  $F_n = 0.72$  and  $0.96$ , respectively). These spectra have approximately similar frequency content although the waveheights were nearly doubled. This effect was achieved by using the same wave tapes and increasing the blower RPM of the **pneumatic** wavemaker.



The spectra provide a random seaway that contains significant energy in the range of the craft natural frequency. This enables an accurate determination of frequency response functions that result from the spectral analysis. Equally important, these spectra may provide a worst case irregular seas condition for the pitch-heave motions of the XR-5 SES in head seas. As can be seen in Figure 10, restriction of motion testing to operation in a "Pierson-Moskowitz" idealized seaway of same wave height to that actually tested would have greatly underpredicted the craft motion since the PM spectrum contains almost all of its energy in the supercritical range of the XR-5.

Figures 11 through 28 present comparisons of the transfer functions obtained from the spectral analysis of the random wave data with those obtained from regular wave experiments. Random wave transfer functions are presented only for frequencies where the pitch-heave coherency was 85% or better to insure confidence in the data. The regular wave experiments at 9 and 12 knots were made with a nominal wave height/wavelength ratio of 1/100, although at longer wave lengths the height was restricted to about one foot because of mechanical limitations of the tow gear. In the 15 knot regular wave runs the nominal wave height was restricted to three inches to minimize the risk to the test apparatus and model. The two circled points in Figure 11 are the points on the pitch transfer function in regular waves where the wave heights are the same as the significant wave heights for the two random seaways. While these two quantities cannot be compared directly, they are among the regular wave points which correlate best with the irregular wave data.

The regular wave transfer functions presented are based on the first harmonic component of the response. In Reference 2 it was shown that the amplitude of the first harmonic is essentially equal to the amplitude based on the total energy, indicating that generation of higher harmonics, which is an indication on nonlinear response, was not a significant factor for all three speeds in waves with lengths greater than the cushion length.

The heave motion data presented in Figures 14 through 16 was derived from slidewire measurements. In Reference 2, data derived from the accelerometer measurements was preferred over the slidewire data because

of high frequency noise produced by flexing of the slidewire pickup. This decision was based on total energy data; however, for the frequencies examined herein, using the first harmonic component from a harmonic analysis, there was no significant difference in the regular wave transfer functions obtained by the two methods. Both signals were again examined in the current evaluation of irregular wave data and the acceleration spectra produced less reliable heave data than did the slidewire measurements for the frequencies of interest because of numerical error introduced in the double integration of the acceleration signal in the frequency domain.

The probability distributions of the double amplitudes of wave height, heave and pitch are presented in Figures 29 through 33. Comparisons of measured histograms with Rayleigh distributions based on the sample variance and on the minimum  $\chi^2$  estimator are presented for each case.

Figure 34 presents transfer functions derived from both regular and irregular wave experiments for a destroyer with a bow bulb (Ship A in Reference 3) at 20 knots in head seas. The random wave results were determined during experiments in a simulated Sea State 5. It is included as an example of the correlation obtained from the two approaches for the more conventional ships.

#### DISCUSSION OF RESULTS

Table 5 presents a summary of the mean values for the random wave experiments. As expected, the mean draft increased and the mean cushion pressure decreased as significant wave height increased. This was a result of the increased cushion air leakage for the more severe sea conditions. Referring to the normalized wave height data, it is seen that the significant wave height varied from 0.27 to 0.69 times the cushion depth providing a range of sea states from relatively mild to severe. (It is not expected that the craft should be able to negotiate sea states with significant wave heights equal to the cushion height at the design Froude number of 0.72)

Figure 5 is a plot of the normalized mean draft and trim data from Table 5 versus the normalized significant wave height. The mean draft/cushion height ratio is presented for the tow point and at the bow. It is seen that the craft sinkage is approximately one-half the significant wave height.

Table 6 presents the significant double amplitude motions determined from the double amplitude distributions and those computed from the measured motion spectra. In all cases, the correlation between the two methods is extremely good. Also included are values computed from the linear superposition of the regular wave transfer functions with the measured wave spectra. Best agreement is seen for heave as would be expected from the examination of the subsequent figures. Agreement is also reasonably good for pitch and relative bow motion.

The significant heave and relative bow motion were normalized by wave height, while the pitch angle in degrees (which is nondimensional) was normalized by wave height/cushion depth. That is, the tabulated pitch angles represent the pitch angle due to a wave height equal to the cushion depth. It is seen that the significant heave as computed from the double amplitude distributions varies from 0.63 to 0.69 times the cushion height while the relative bow motion varied from 1.6 to 2.2 times the cushion height. That is to say, there is some attenuation of heave, while the relative bow motion is amplified. The attenuation of heave with respect to wave height did not vary significantly with speed, although the relative bow motion amplification decreased with speed. The significant pitch angles (computed from the double amplitude distributions) vary from 4.9 degrees at the highest speed to 9.4 at the lowest (design) speed. The variation in normalized response for runs at the same Froude number give an indication of the nonlinearity of the response. For example, one sees that the normalized heave varies from 0.69 to 0.65 at the Froude number of 0.72 for the moderate and the severe sea state, respectively, indicating that the nonlinear effect is relatively weak.

It is evident from Table 6 that the significant responses calculated in three different ways agree reasonably well, generally within about 10 percent. This implies that significant heave, pitch and relative bow motion can be predicted within engineering accuracy using linear superposition for the speeds and sea states of the order of those investigated here. The generally good agreement of responses computed from the double amplitude distributions to those computed from the power spectra implies that the random processes are sufficiently narrow-banded and Gaussian.



Table 7 presents the significant double amplitude accelerations at the bow and at the center of gravity in a form similar to Table 6. The acceleration data have been normalized in Table 7 so that they represent the acceleration due to a significant wave height equal to the cushion height. For example, to compute the acceleration for a wave height of one-half the cushion height, multiply the linearized acceleration response by one-half. Furthermore, one can compare the normalized accelerations at the same Froude number for the two lower speeds where tests were made in wave spectra of different severities. One sees that there is considerable amplitude dependence for the 0.96 Froude number, although the amplitude dependence at the design Froude number of 0.72 is relatively small.

Another indication of nonlinear effects on the accelerations can be obtained from comparison of significant responses computed from the double amplitude distributions to those computed using the linear superposition assumption. One sees that the response levels computed using linear superposition consistently underpredict the motions obtained from the double amplitude distributions. (The significant levels computed from the double amplitude distributions may be considered the "correct" or reference values, as these are direct statistical observations that are not dependent upon any assumptions about the nature of the responses). The amount of underprediction was found to be related to the severity of the sea state. This is illustrated in Figure 6 where the ratio of significant acceleration levels derived using the linear superposition assumption to the double amplitude distribution values is plotted against normalized significant wave height. This ratio decreases with severity of sea state. One sees that the heave acceleration is underpredicted by a factor of 30 to 40 percent using linear superposition. The nonlinear effect on bow acceleration is more sensitive to sea state, the amount of underprediction varying from 10 to 40 percent. One may use linear superposition to estimate acceleration levels for XR-5 type craft, provided the speed and sea state is within the range of the available data, by using Figure 6. That is, the curves in Figure 6 represent correction factors for bow and heave acceleration. For example, if one is computing acceleration levels for a significant wave height of one-half the cushion depth, the correct factors are 0.64 and 0.78 for heave and bow acceleration, respectively.

To correct for the nonlinear effect one divides the response level derived from the linear superposition assumption by the correction factor. This should give a result accurate enough for engineering purposes.

Figures 11 through 13 present plots of pitch angle per unit wave slope as a function of encounter frequency for Froude numbers of 0.72, 0.96 and 1.20. Correlation is reasonably good for all conditions. At a Froude number of 0.96 the regular wave transfer function correlated best with those of the more severe sea condition.

Figures 14 through 16 show excellent correlation between transfer functions of heave motion as a function of encounter frequency for all conditions.

Figures 17 through 19 present the transfer functions of relative bow motion obtained from the bow sonic measurements. Reasonable correlation is seen for all conditions.

Figures 20 through 22 present bow acceleration per unit wave height as a function of encounter frequency. Reasonable correlation again generally exists, looking best in the low frequency range. Figures 23 through 25 present similar results for heave acceleration derived from accelerometer data. The overall correlation is as good as that for the bow acceleration data, with the best correlation existing at low frequencies. At Froude number of 0.72 the regular wave data correlates best with the more severe sea condition.

Figures 26 through 28 present plots of stern seal motion per unit relative stern displacement. Correlation is very good at 9 knots, reasonably good at 12 knots but some discrepancies appear at high frequencies for 15 knots.

The experimental motion histograms in Figures 29 through 33 exhibit reasonable agreement with the computed Rayleigh distributions although several discrepancies are evident. Experimental histograms of wave height show a less than desired agreement with the computed Rayleigh distributions for the lower sea conditions.

Figure 34 is included in order to provide the reader with a measure for assessing the degree of correlation between the regular and irregular wave approach for determining transfer functions for the high L/B craft.

This figure, from Reference 3, provides an indication of the correlation generally obtained for conventional hull forms. It presents transfer functions derived from both regular and irregular wave experiments for a destroyer with a bow bulb (Ship A in Reference 3) at 20 knots in head seas. The random wave results were determined during experiments in a simulated Sea State 5.

#### SUMMARY AND CONCLUSIONS

Motions data have been presented for the XR-5 model in random head waves for several sea conditions and for three speeds corresponding to Froude numbers of 0.72, 0.96 and 1.20.

Transfer functions derived from the random wave experiment were presented that show reasonable agreement with those derived from the regular wave experiments in References 1 and 2. Furthermore, computations of significant values based on the linear superposition of regular wave transfer functions with the measured wave spectra correlate very well with the corresponding measured random wave responses for the motions though the accelerations were underpredicted.

The data also provides an indication of the behavior of the XR-5 in an irregular sea where the wave spectra contain significant energy in the range of the natural frequency of the craft. It is evident that restricting the investigation to Pierson-Moskowitz spectra with the same significant wave height would result in a less severe condition for the XR-5 than that examined here. Analysis of mean draft and trim in these more severe seas indicated that the craft sinkage was approximately one-half the significant wave height.

Comparisons of experimental histograms with Rayleigh distributions derived from measured statistical properties show acceptable agreement for heave and pitch provided that the wave height exhibits reasonable Rayleigh behavior.

In summary, the results presented show that for engineering purposes the prediction of rigid body motions (and, to some extent, accelerations) for the high length/beam ratio SES craft by application of the principle of superposition can be performed with reasonable accuracy for the speeds and sea states examined here.



#### ACKNOWLEDGMENTS

The authors wish to acknowledge the guidance and assistance of Ms. M.D. Ochi in the design of the model experiments and in the interpretation of the results. Appreciation is expressed to Dr. D. Moran and Mr. J. Kallio for planning and supervision of the experiments. Appreciation is expressed to Mr. M. Davis for his work in performing the data reduction. The authors wish to acknowledge the assistance during the experiments of Messrs. J. Bonilla-Norat, J. Fein, M. Pemberton and B. Peters.

#### REFERENCES

1. Magnuson, A.H. and Wolff, K.K., "Seakeeping Characteristics of the XR-5, A High Length-Beam Ratio Manned Surface Effect Testcraft:  
1. XR-5 Model Response in Regular Head Waves," Ship Performance Department Report SPD 616-01, March 1975
2. Magnuson, A.H. and Wolff, K.K., "Seakeeping Characteristics of the XR-5, A. High Length-Beam Ratio Manned Surface Effect Testcraft  
2. Results of Linearity Investigation, Effects of Changes from Reference Operating Condition and Trim and Draft in Regular Waves", Ship Performance Department SPD 616-02, March 1975
3. Cox, G.C. and Gerzina, D.M., "A Comparison of Predicted and Experimental Seakeeping Characteristics for Ships with and Without Large Bow Bulbs", Ship Performance Department Report SPD 591-01, November 1974.

TABLE 1  
HIGH L/B SES MODEL CHARACTERISTICS

<u>Symbol</u>		<u>Dimensions Model Scale</u>	
LOA	Length Overall	15.58 ft	4.75 m
-	Design Displacement	275.0 lbs	124.74 kg
-	Test Displacement	298.0 lbs	135.17 kg
L	Length of Bubble	13.83 ft	4.22 m
B	Beam of Bubble	2.12 ft	0.65 m
L/B	Ratio	6.54	6.54
TCG	Transverse Center of Gravity	£	£
VCG	Vertical Center of Gravity (Above Keel Line)	0.90 ft	0.27 m
LCG	Longitudinal Center of Gravity (Forward of Transom)	7.21 ft	2.20 m
K	Radius of Gyration (in Pitch)	4.71 ft	1.44 m
K/LOA	Ratio	0.30	0.30
Tow Point Forward of Transom		9.63 ft	2.94 m
Tow Point Above Keel Line		0.97 ft	0.30 m

TABLE 2  
TRANSDUCER LOCATIONS ON MODEL

<u>Transducer or Reference Point</u>	<u>Forward of the Transom</u>	
	<u>Feet</u>	<u>Meters</u>
Wave Height Probe (Carriage Borne)	51.125	15.583
Relative-Range (Sonic) Probe #1 (RBM)	15.911	4.850
Bow	15.580	4.749
Trailing Edge of Bow Seal	14.163	4.317
Relative-Range (Sonic) Probe #2	13.109	3.996
Pitch Heave Staff	9.625	2.934
Relative-Range (Sonic) Probe #3	7.974	2.430
Longitudinal Center of Gravity	7.208	2.197
Relative-Range (Sonic) Probe #4	2.588	0.789
Trailing Edge of Stern Seal	0.333	0.102
Transom	0	0
Relative-Range (Sonic) Probe #5 (RSM)	-0.229	-0.070

TABLE 3  
OPERATING CONDITIONS FOR MODEL

Fan Configuration: 2-0-2 (Two fans in forward seal, none in main plenum, and two in stern seal)

Downstop Settings: All Downstops at maximum downward position

Duct Valve Settings: (Orifice Areas)

Main Bow Seal	4 in <sup>2</sup>	25.81 cm <sup>2</sup>
Third Lobe, Bow	0.625 in <sup>2</sup>	4.03 cm <sup>2</sup>
Main Stern Seal	5.5 in <sup>2</sup>	35.49 cm <sup>2</sup>
Third Lobe, Stern	4 in <sup>2</sup>	25.81 cm <sup>2</sup>



TABLE 4

SPEED IN KNOTS FOR VARIOUS SCALE RATIOS  
OF XR-5 HIGH L/B SES, AS A FUNCTION  
OF FROUDE NUMBER

$F_n = \frac{U}{\sqrt{gL}}$	Tow Tank Model (Scale ratio = 1/3)	Manned Testcraft (Scale ratio = 1)	Proposed Ship (Scale ratio = 10.667)
0.48	6	10.4	40
0.72	9	15.6	51
0.96	12	20.8	68
1.20	15	26.0	85



TABLE 5

## SUMMARY OF RANDOM WAVE CONDITIONS

XR-5 MODEL  
HEAD SEAS

$F_n$	SIGNIFICANT WAVE HEIGHT/ CUSHION DEPTH	SAMPLE TIME (MINUTES)	MEAN TRIM BOW UP (DEGREES)	MEAN DRAFT AT TOW POINT/CUSHION DEPTH	MEAN CUSHION PRESSURE NEAR BOW (PSFG)	MEAN CUSHION PRESSURE NEAR STERN (PSFG)
0.72	0.392	1.82	2.19	0.439	8.40	8.30
0.72	0.529	2.80	2.17	0.498	7.53	7.48
0.96	0.309	2.85	2.32	0.414	8.53	8.37
0.96	0.693	2.20	2.20	0.547	7.03	6.03
1.20	0.267	1.22	2.30	0.469	8.18	7.89

$F_n$	SIGNIFICANT WAVE HEIGHT/ CUSHION DEPTH	CYCLES OF WAVES ENCOUNTERED	MEAN CUSHION PRESSURE NEAR BOW (PASCALS GAGE)	MEAN CUSHION PRESSURE NEAR STERN (PASCALS GAGE)
0.72	0.392	167	402.2	397.4
0.72	0.529	246	360.5	258.1
0.96	0.309	302	408.4	400.8
0.96	0.693	202	336.6	288.7
1.20	0.267	138	391.7	377.8

TABLE 6  
SIGNIFICANT DOUBLE AMPLITUDE MOTIONS  
XR-5 MODEL  
HEAD SEAS

Fn	SIGNIFICANT WAVE HEIGHT/ CUSHION DEPTH	SIGNIFICANT HEAVE/ SIG. WAVEHEIGHT			SIGNIFICANT PITCH (SIG. WAVEHEIGHT/ CUSHION DEPTH)			SIGNIFICANT RBM/ SIG. WAVEHEIGHT		
		DA <sup>1</sup>	PS <sup>2</sup>	LS <sup>3</sup>	DA	PS	LS	DA	PS	LS
0.72	0.392	0.692	0.682	0.657	9.06	9.11	8.06	2.24	2.19	1.84
0.72	0.529	0.650	0.642	0.635	9.36	8.87	8.20	2.06	1.97	1.84
0.96	0.309	0.684	0.662	0.663	6.25	6.25	6.28	1.83	1.94	1.78
0.96	0.693	0.689	0.717	0.731	6.88	7.01	6.75	1.64	1.68	1.76
1.20	0.267	0.626	0.682	0.656	4.93	5.08	5.57	1.62	1.75	1.79

<sup>1</sup> Significant response computed from double amplitude distributions

<sup>2</sup> Significant response computed from spectra analysis

<sup>3</sup> Significant response computed from linear superposition of regular wave transfer functions with the corresponding measured wave spectra

TABLE 7  
SIGNIFICANT DOUBLE AMPLITUDE ACCELERATIONS  
XR-5 MODEL  
HEAD SEAS

Fn	SIGNIFICANT WAVE HEIGHT PER UNIT CUSHION DEPTH	SIGNIFICANT BOW ACCELERATION (G's) FOR A WAVEHEIGHT EQUAL TO THE CUSHION DEPTH			SIGNIFICANT CG ACCELERATION (G's) FOR A WAVEHEIGHT EQUAL TO THE CUSHION DEPTH		
		DA	PS	LS	DA	PS	LS
0.72	0.392	1.99	2.07	1.66	0.71	0.75	0.46
0.72	0.529	2.12	2.08	1.64	0.74	0.77	0.45
0.96	0.309	1.91	2.11	1.52	0.84	1.01	0.58
0.96	0.693	2.48	2.63	1.52	0.95	1.09	0.58
1.20	0.267	1.95	2.30	1.72	1.05	1.24	0.67

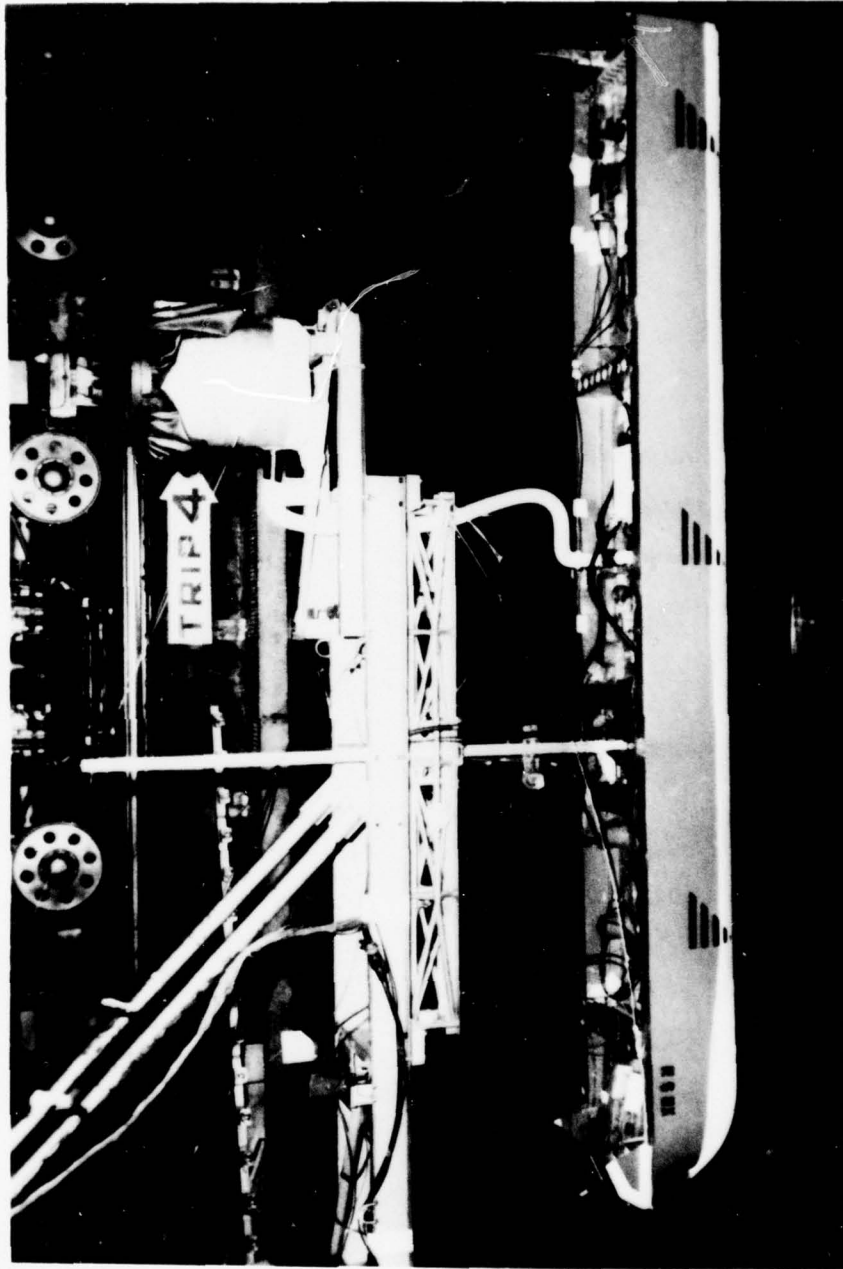


Figure 1 - Side View of Model and Towing Gear with Model Clear of Water



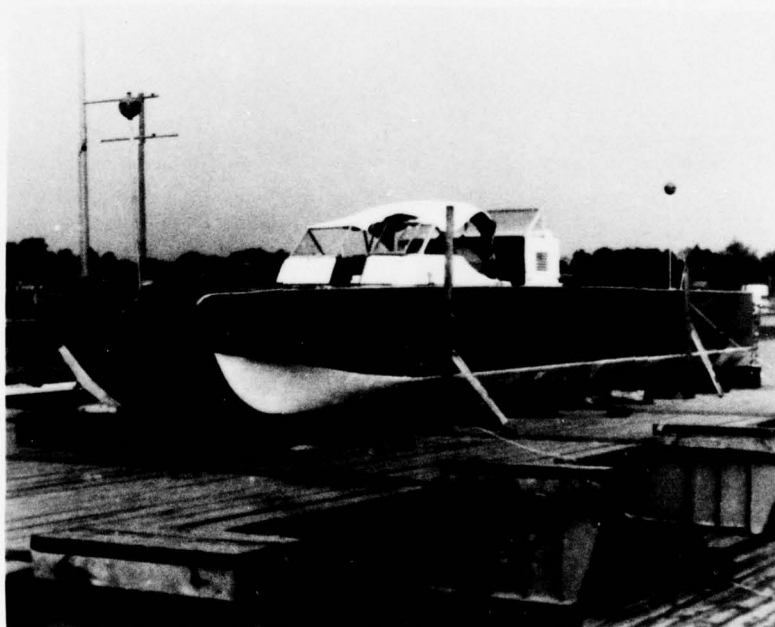
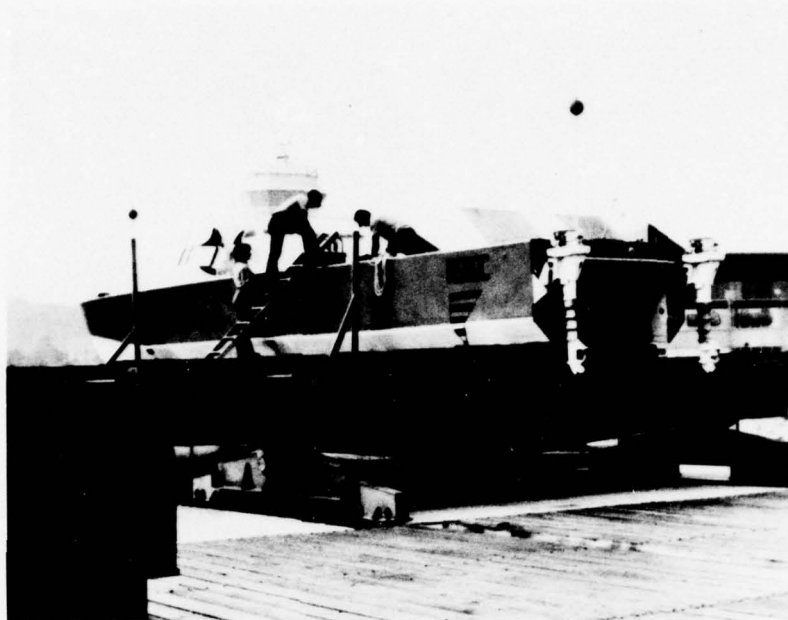


Figure 2 - The XR-5 Manned Testcraft

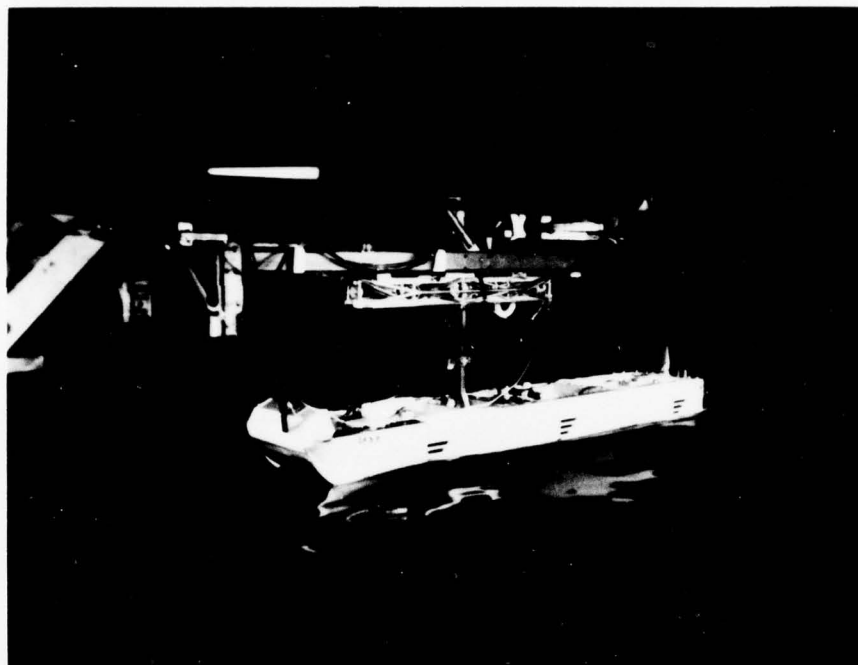


Figure 3 - XR-5 Model in Random Waves:  $F_n = 0.96$ ,  
Sig. W.H./Cushion Depth =  $.309^n$

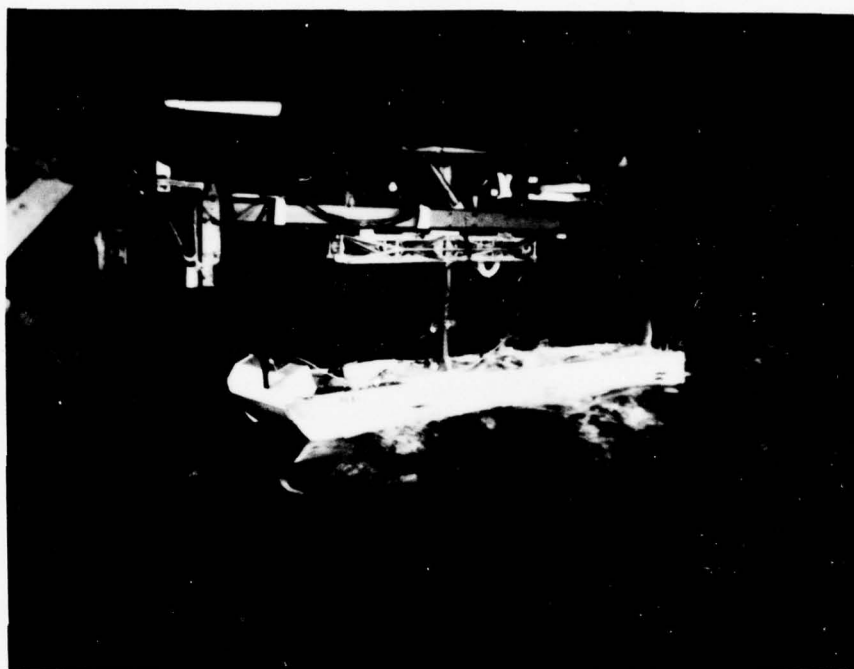


Figure 4 - XR-5 Model in Random Waves:  $F_n = 0.96$ ,  
Sig. W.H./Cushion Depth =  $.693^n$

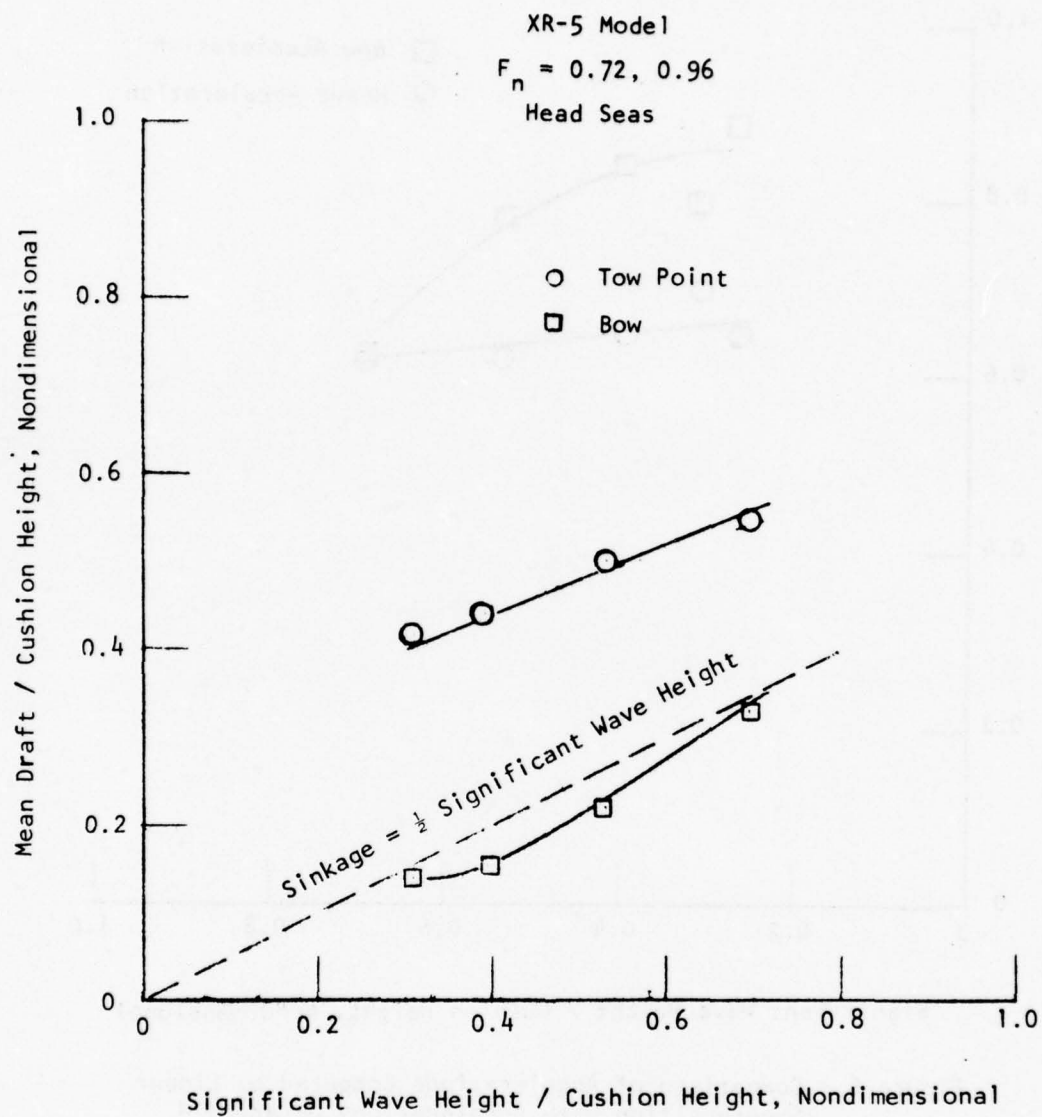


Figure 5 - Mean Draft in Irregular Waves



XR-5 Model  
 $F_n = 0.72, 0.96$   
Head Seas

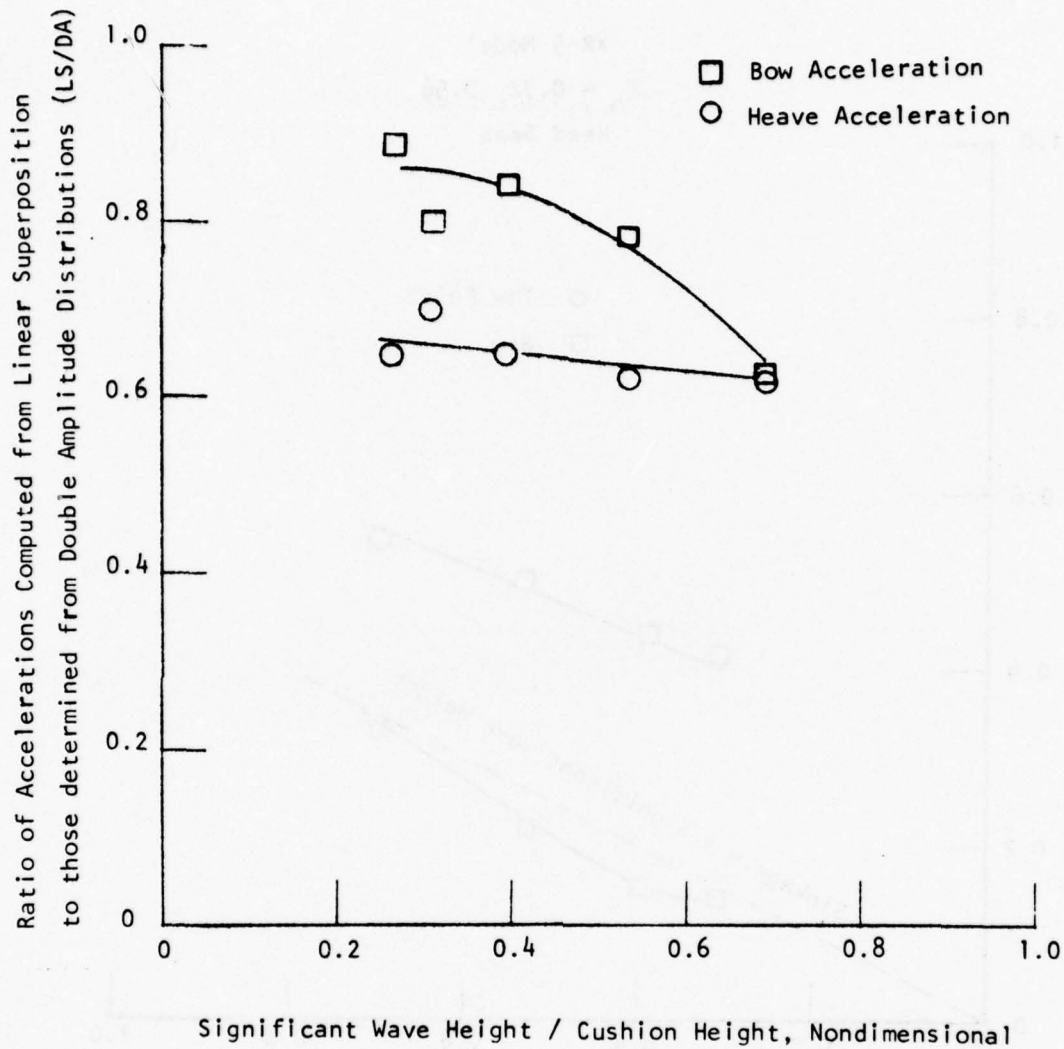


Figure 6 - Comparison of Accelerations Computed by Linear Superposition with Accelerations Determined from Double Amplitude Distributions

XR-5 Model

9 Knots

Head Seas

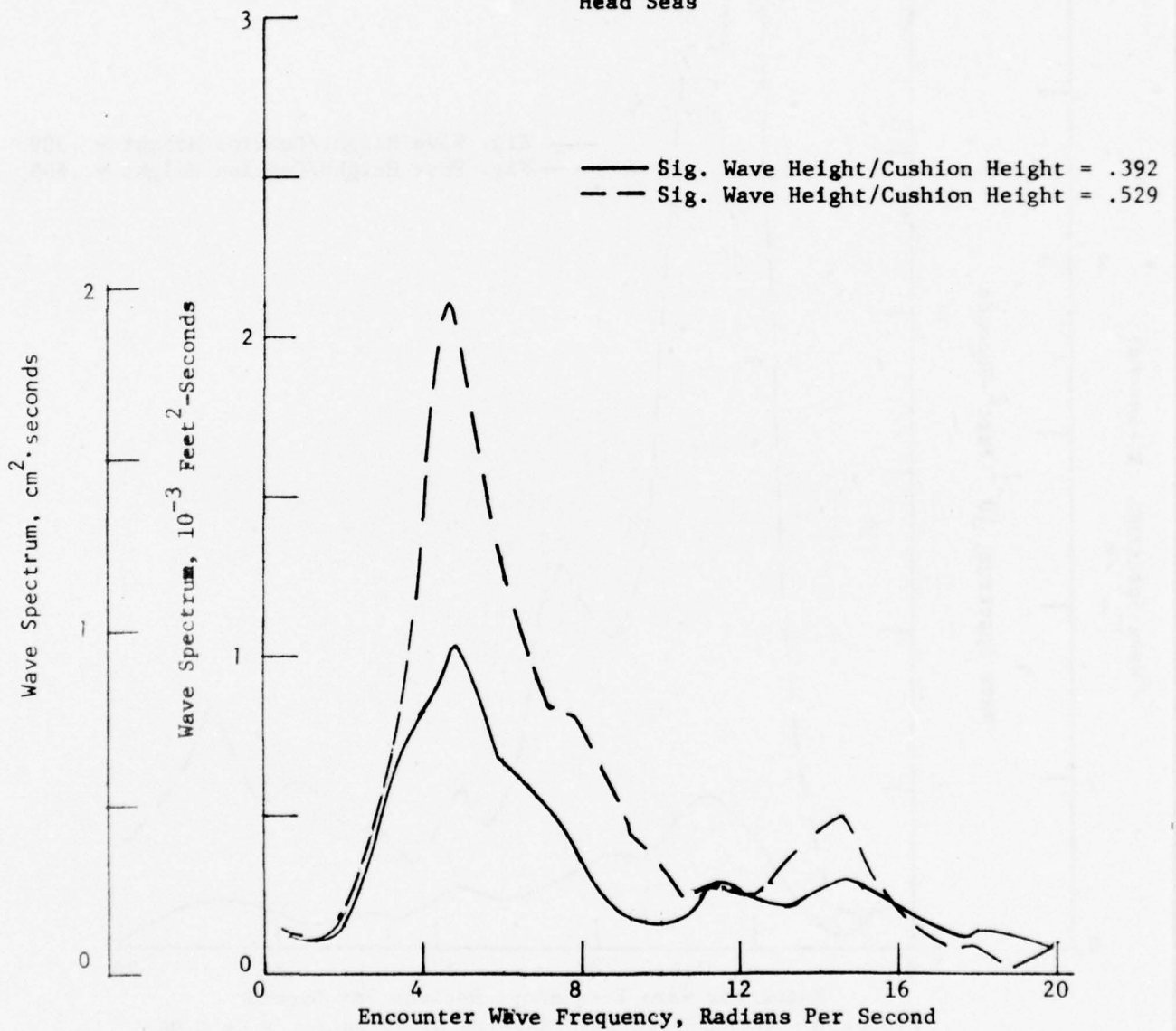


Figure 7 - Encountered Wave Spectra at 9 Knots,  $F_n = 0.72$

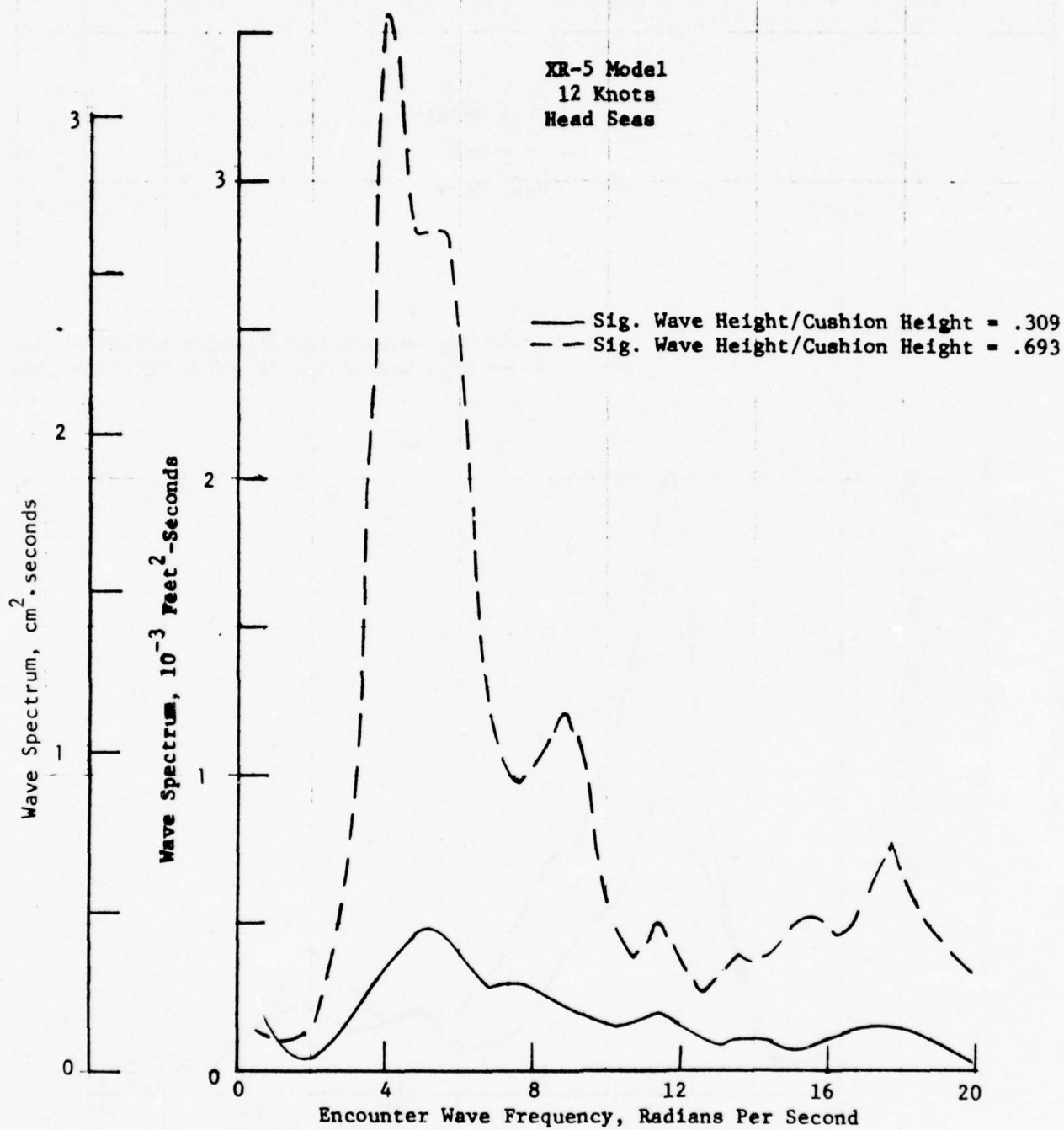


Figure 8 - Encountered Wave Spectra at 12 Knots,  $F_n = 0.96$

XR-5 Model  
15 Knots  
Head Seas

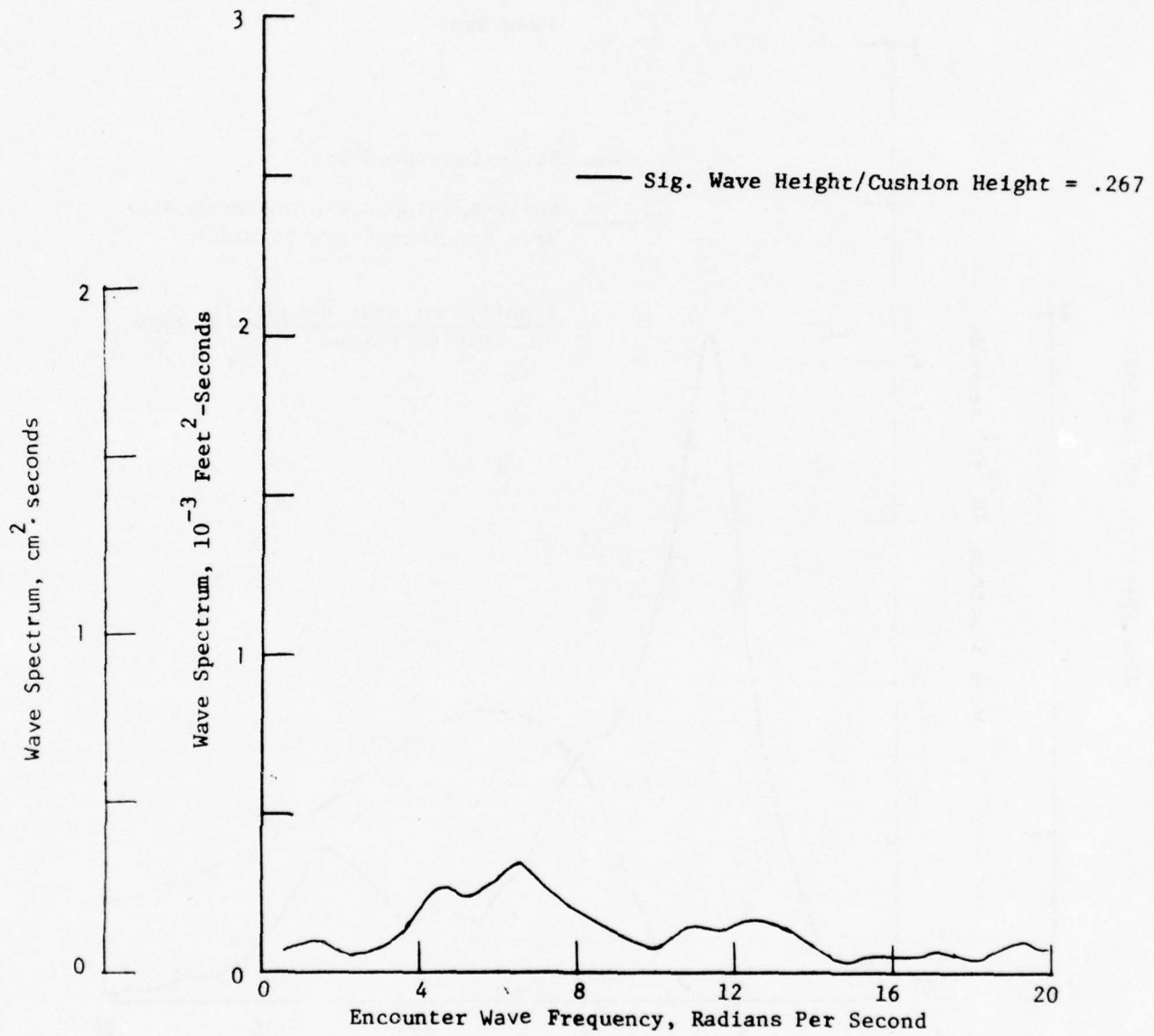


Figure 9 - Encountered Wave Spectra at 15 Knots,  $F_n = 1.20$



XR-5 Model

9 Knots

Head Seas

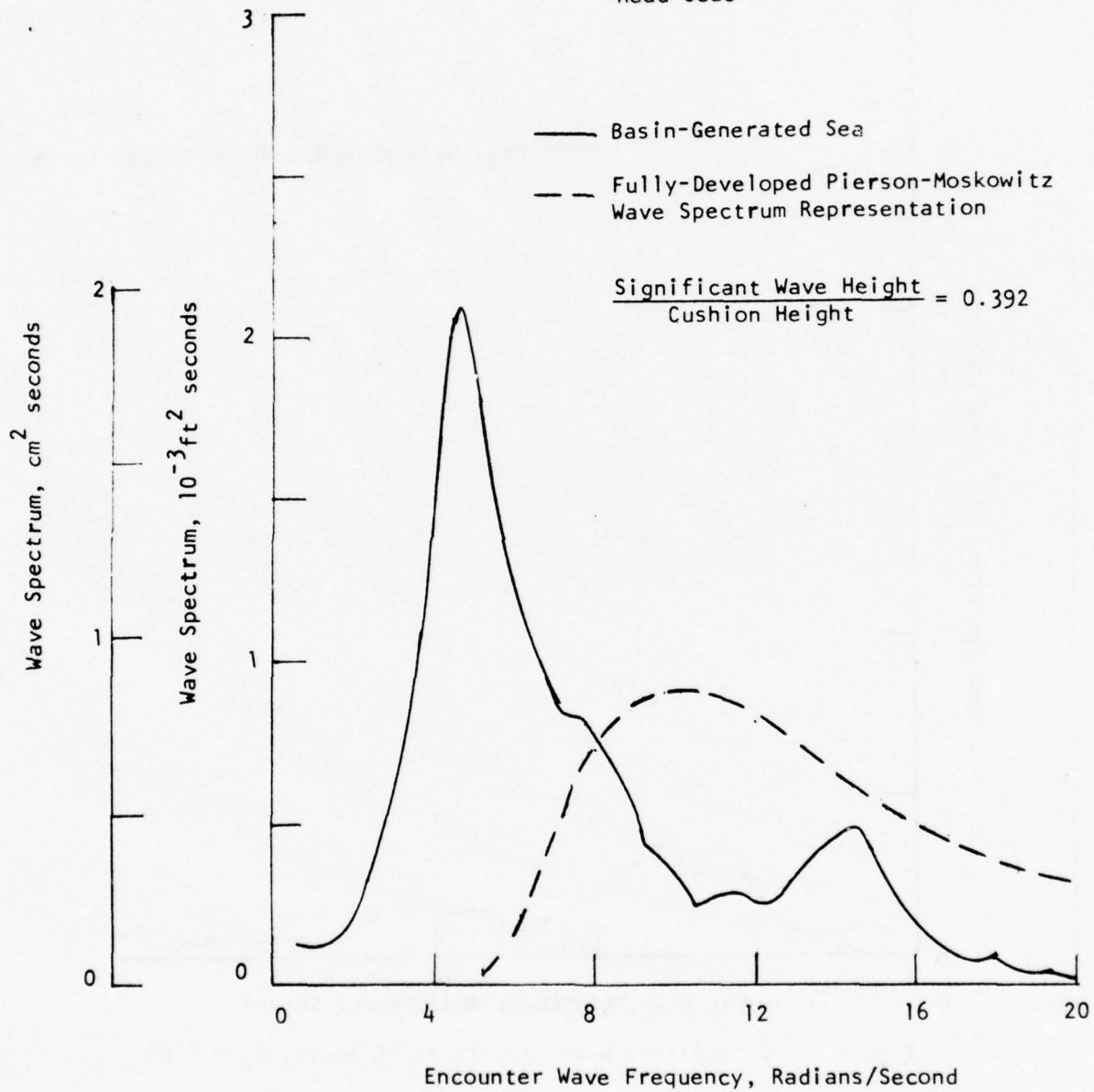


Figure 10 - Comparison of Basin-Generated Spectrum with Pierson-Moskowitz Spectrum

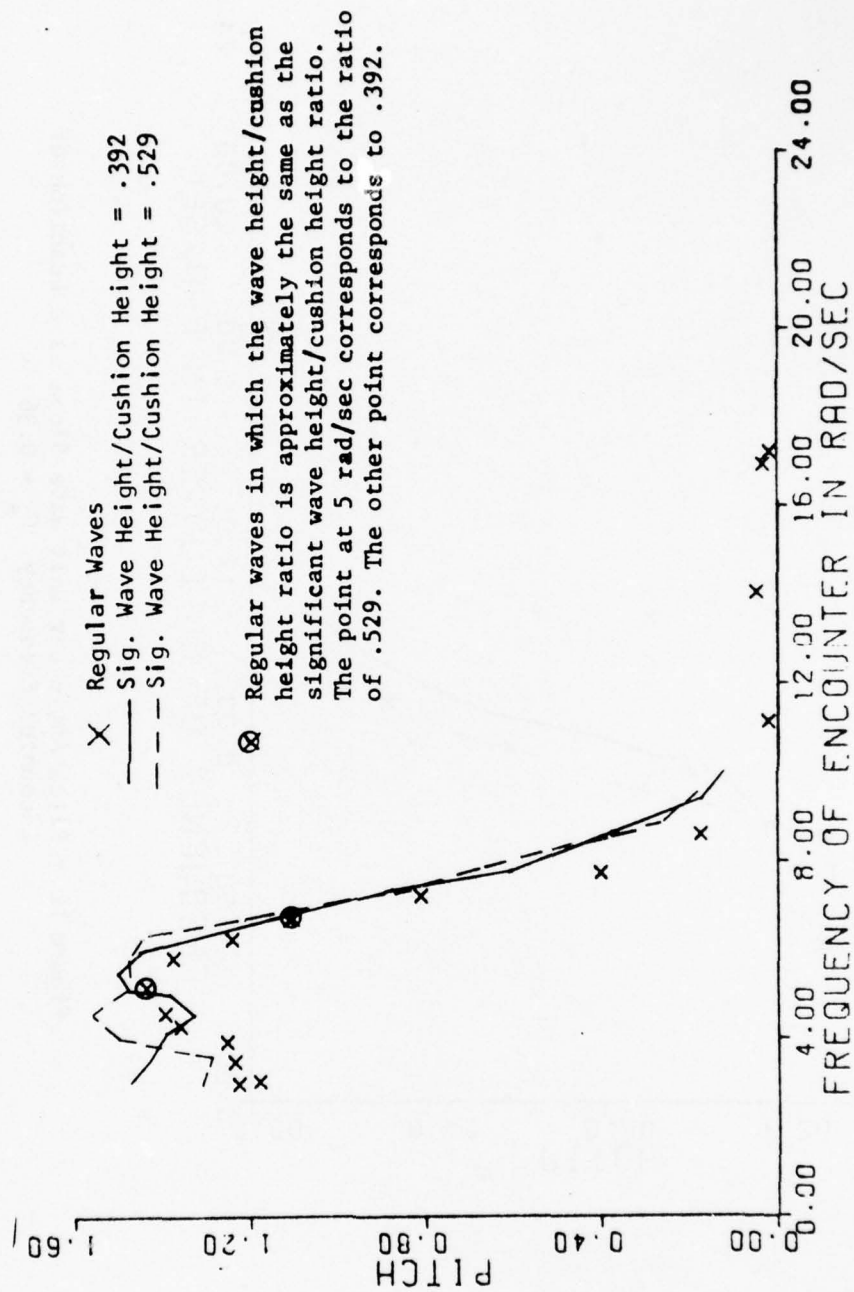


Figure 11 - Pitch Angle per Unit Wave Slope as a Function of Encounter Frequency,  $F_n = 0.72$

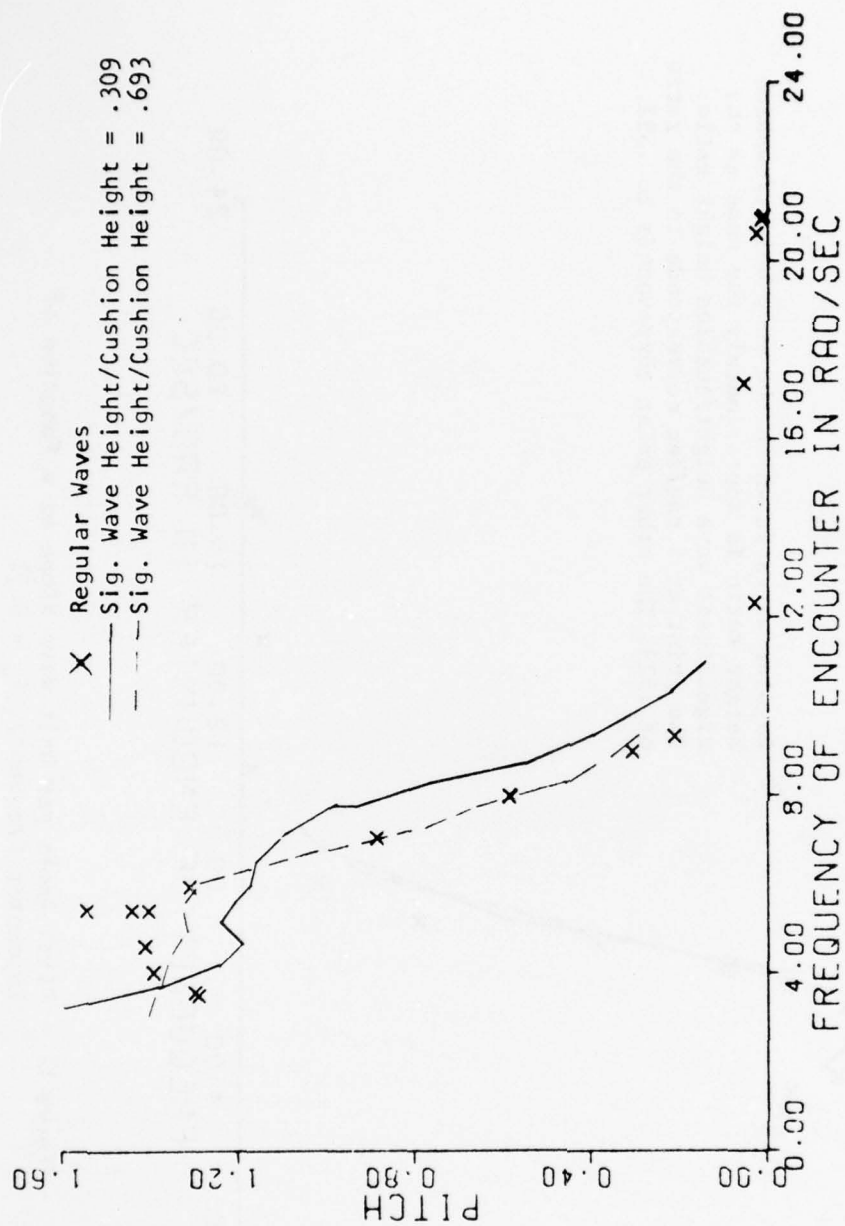


Figure 12 - Pitch Angle per Unit Wave Slope as a Function of Encounter Frequency,  $F_n = 0.96$

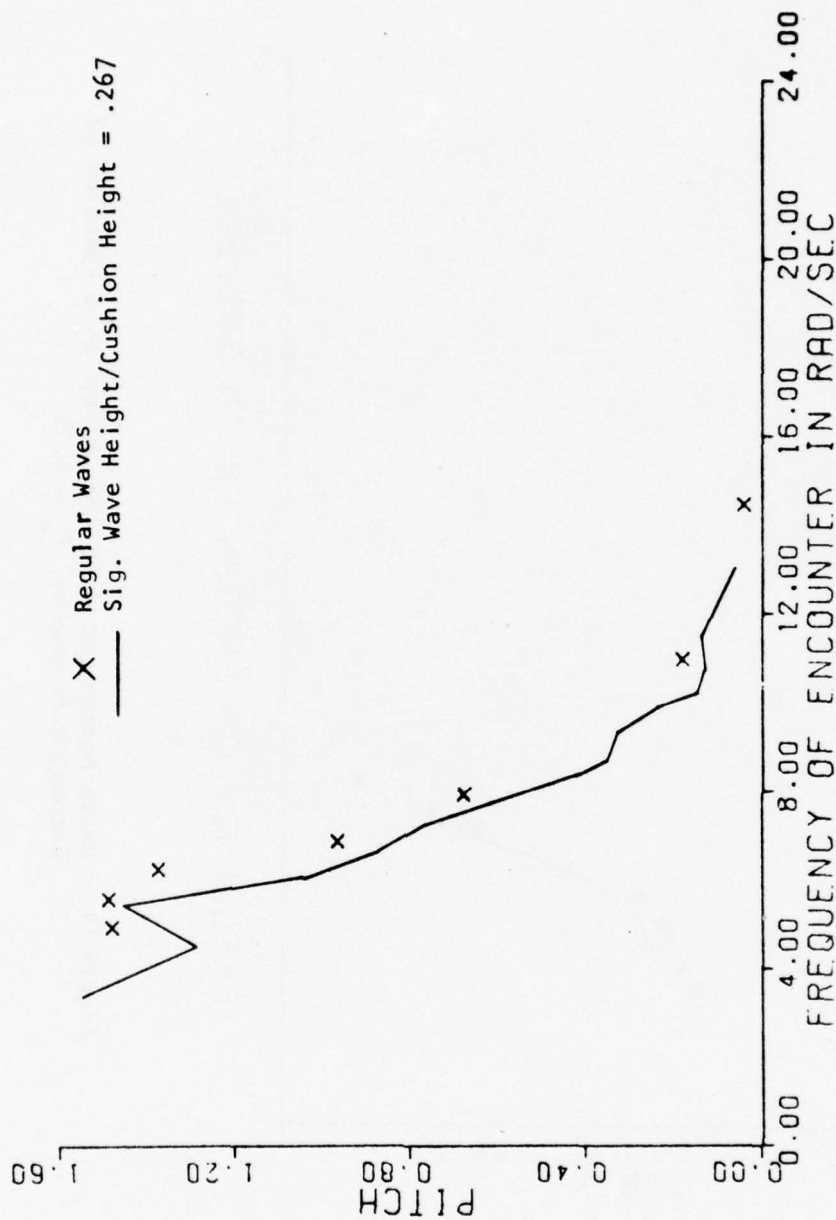


Figure 13 - Pitch Angle per Unit Wave Slope as a Function of Encounter Frequency,  $F_n = 1.20$



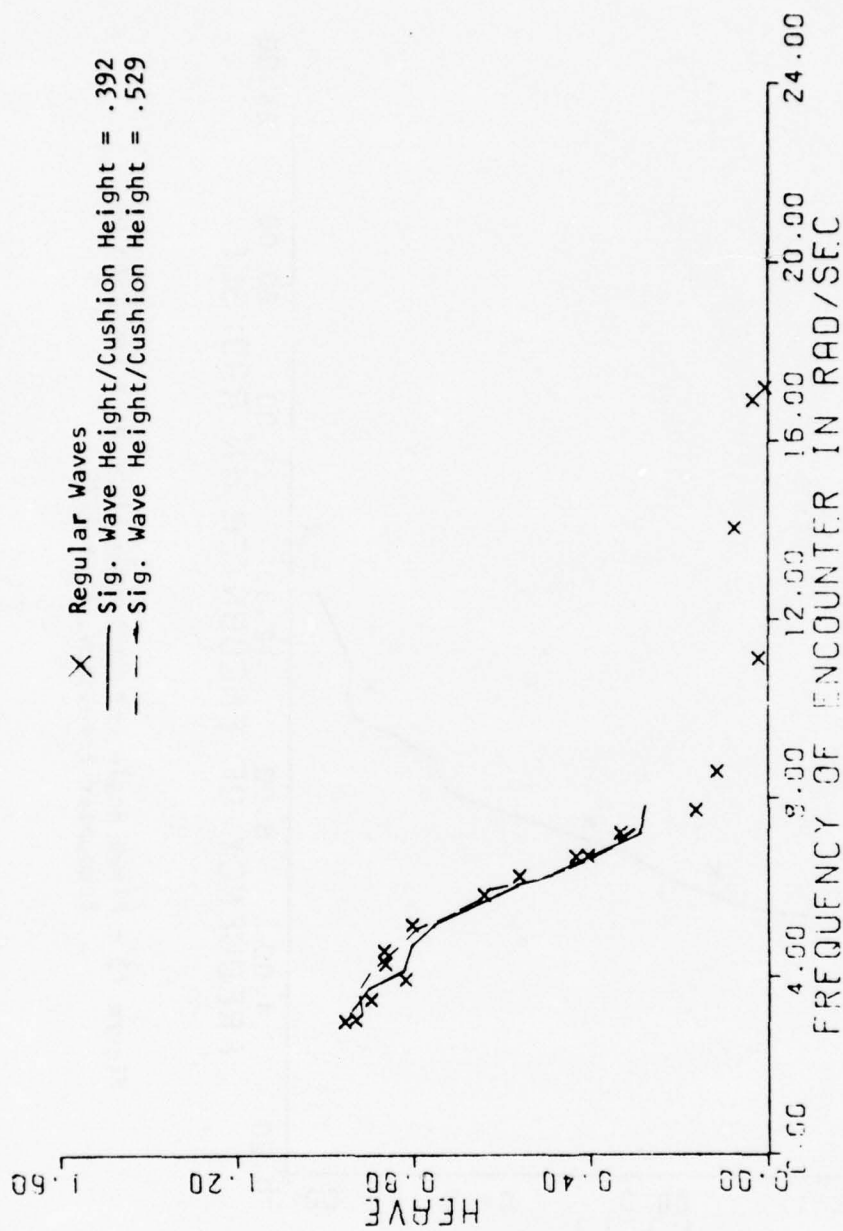


Figure 14 - Heave Motion per Unit Wave Height as a Function of Encounter Frequency,  $F_n = 0.72$

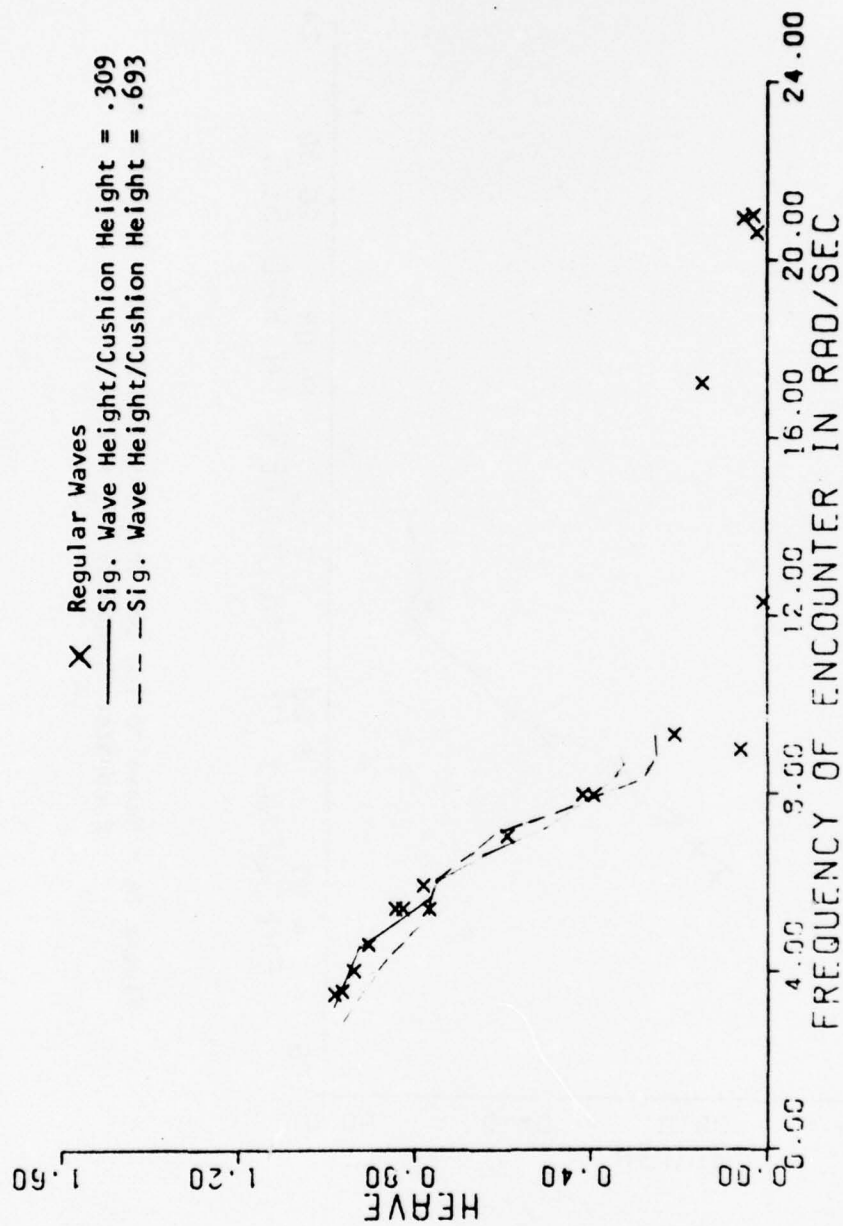


Figure 15 - Heave Motion per Unit Wave Height as a Function of Encounter Frequency,  $F_n = 0.96$

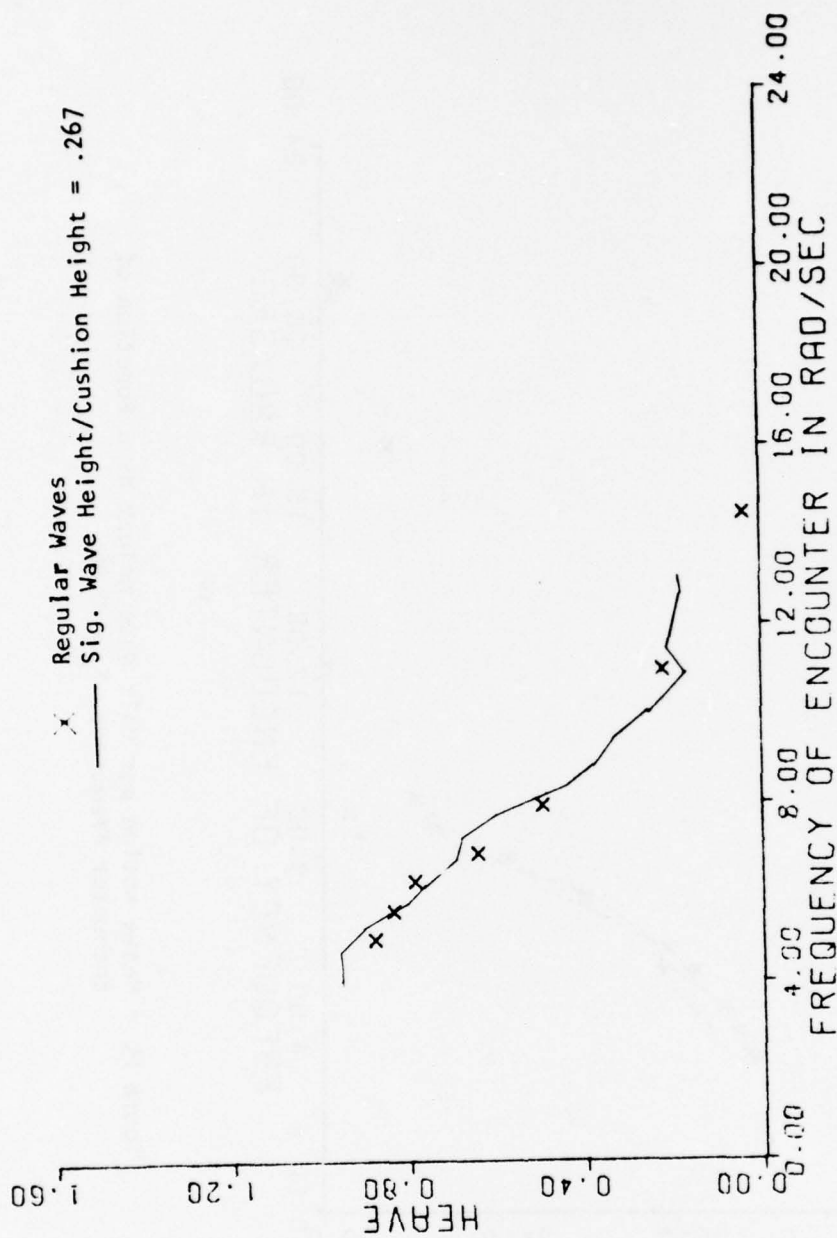


Figure 16 - Heave Motion per Unit Wave Height as a Function of  
 Encounter Frequency,  $F_n = 1.20$

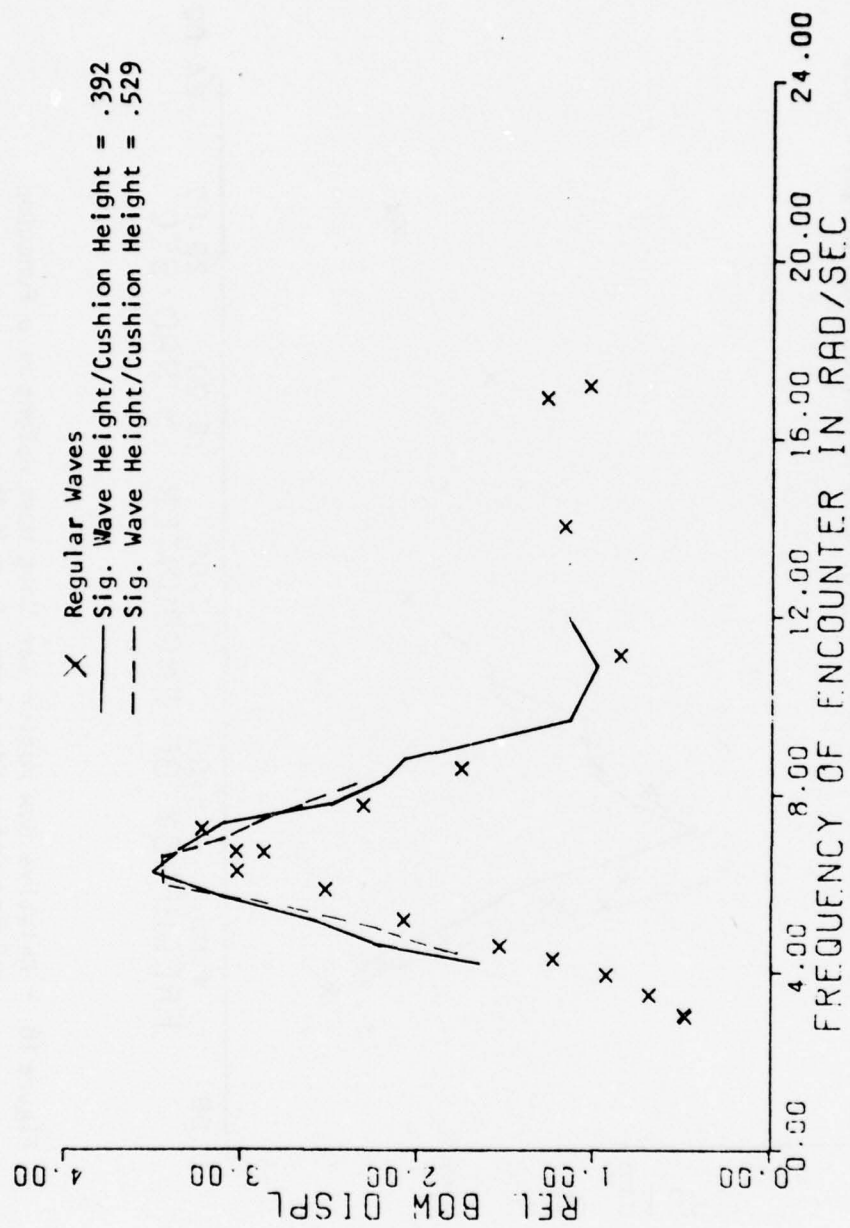


Figure 17 - Relative Bow Motion per Unit Wave Height as a Function of Encounter Frequency,  $F_n = 0.72$

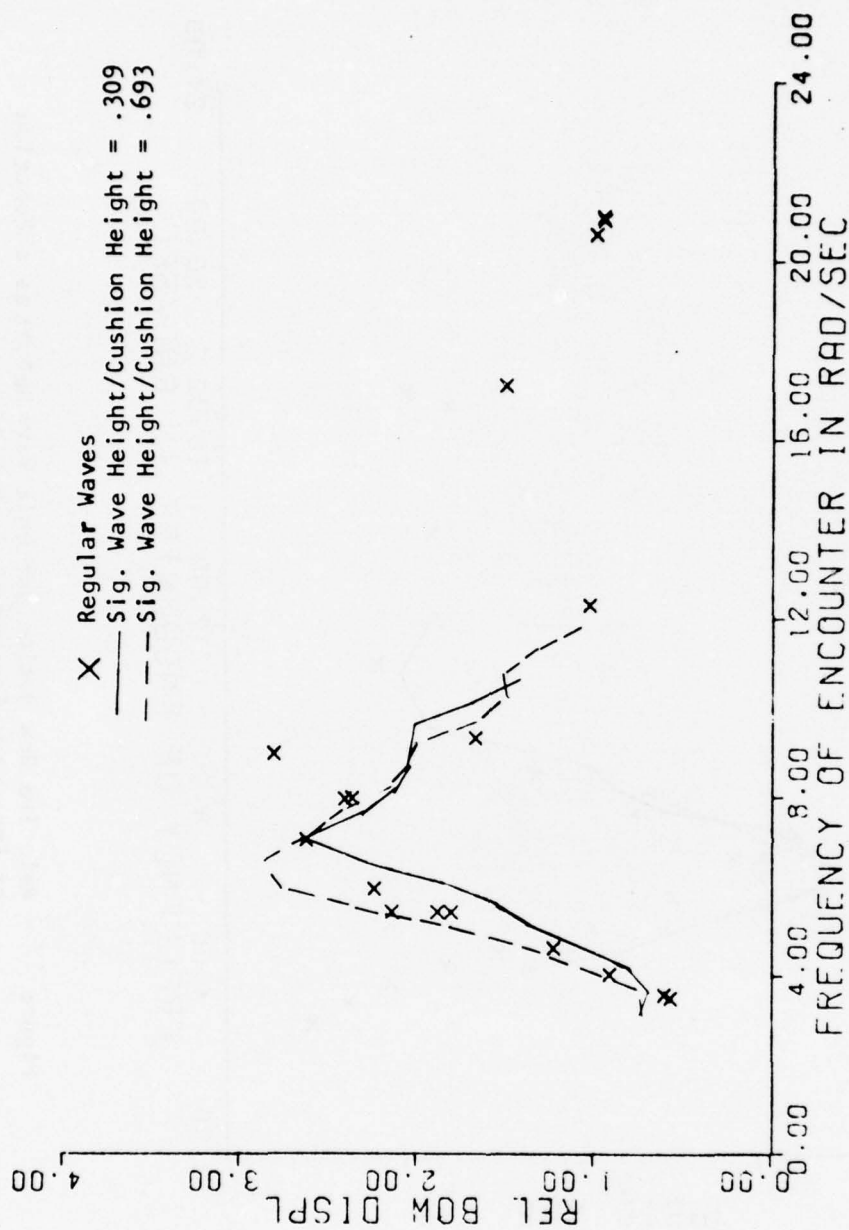


Figure 18 - Relative Bow Motion per Unit Wave Height as a Function of Encounter Frequency,  $F_n = 0.96$



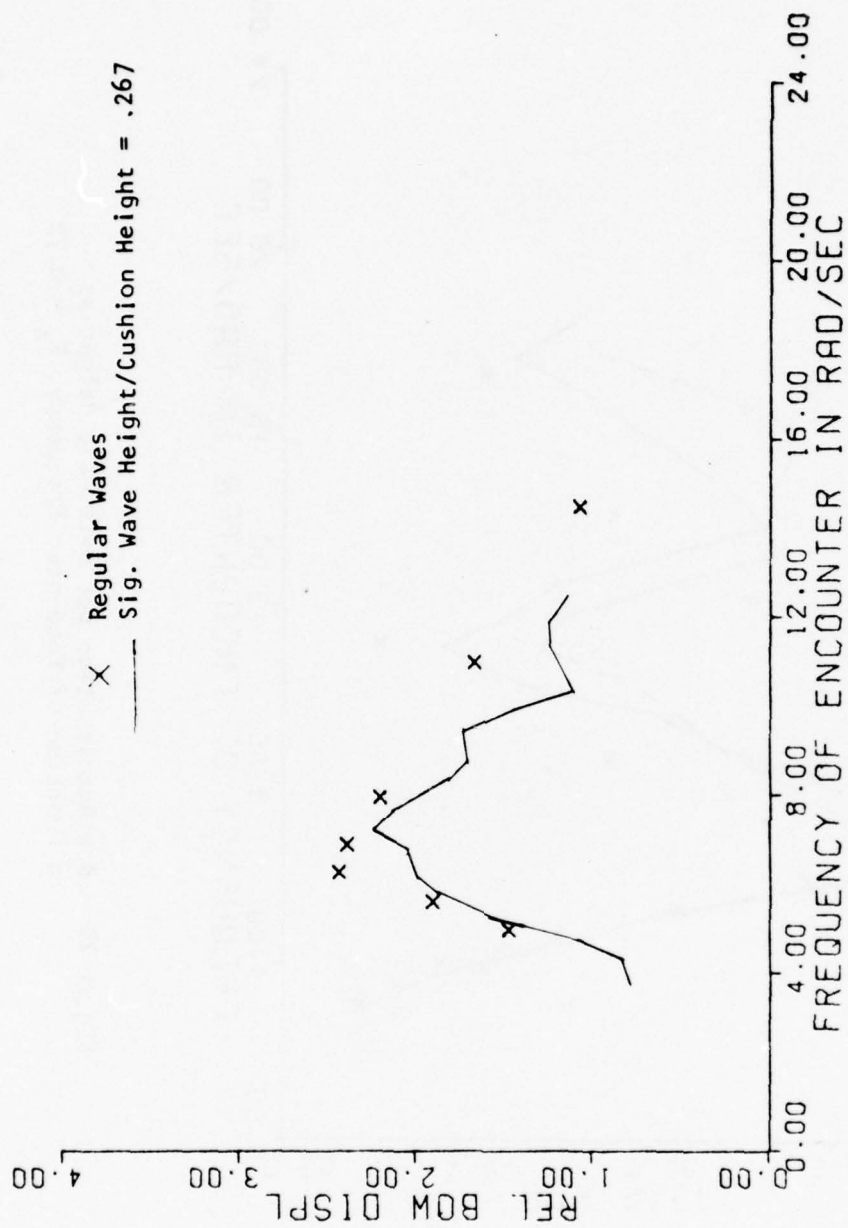


Figure 19 - Relative Bow Motion per Unit Wave Height as a Function of Encounter Frequency,  $F_n = 1.20$

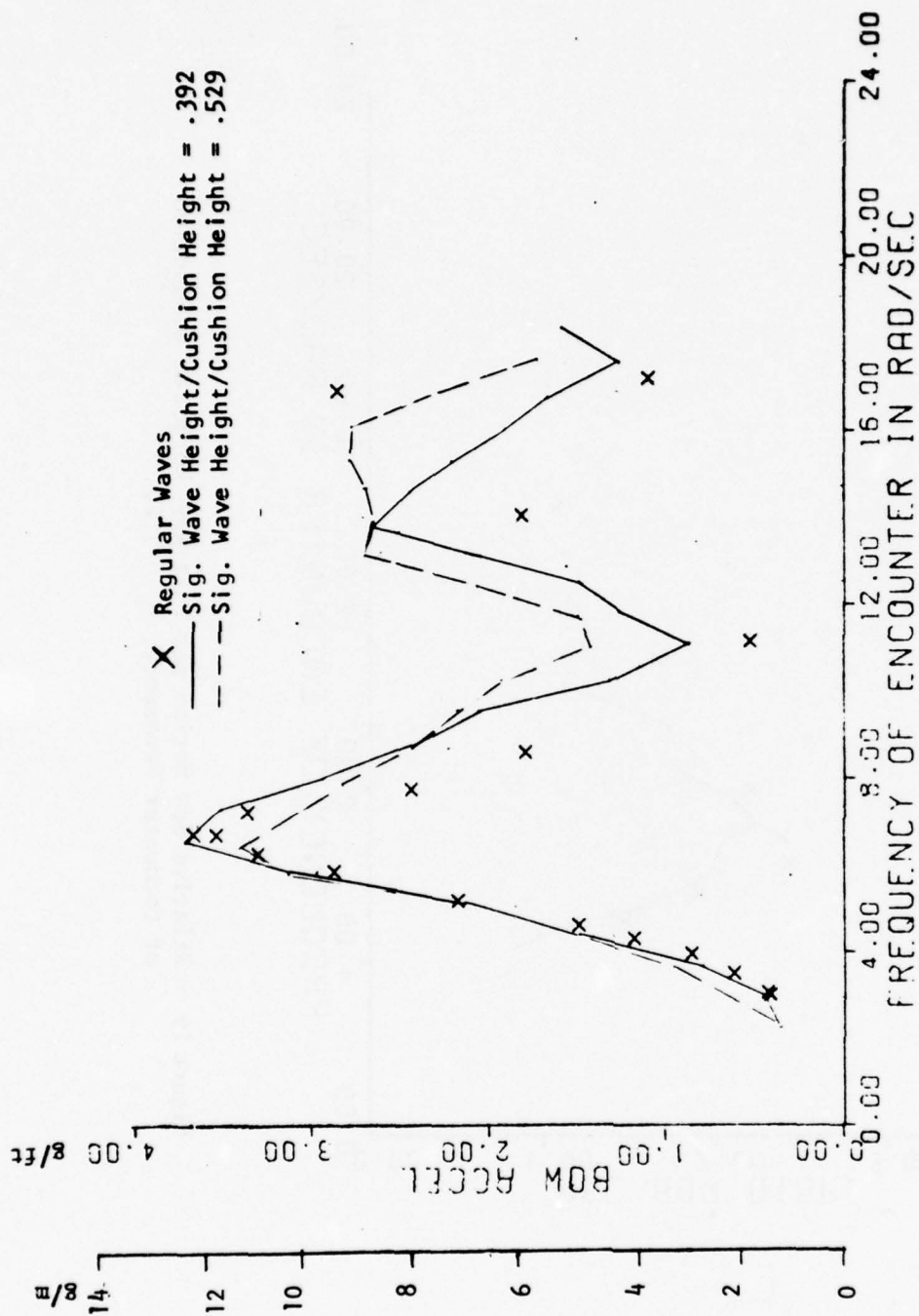


Figure 20 - Bow Acceleration per Unit Wave Height as a Function of Encounter Frequency,  $F_n = 0.72$

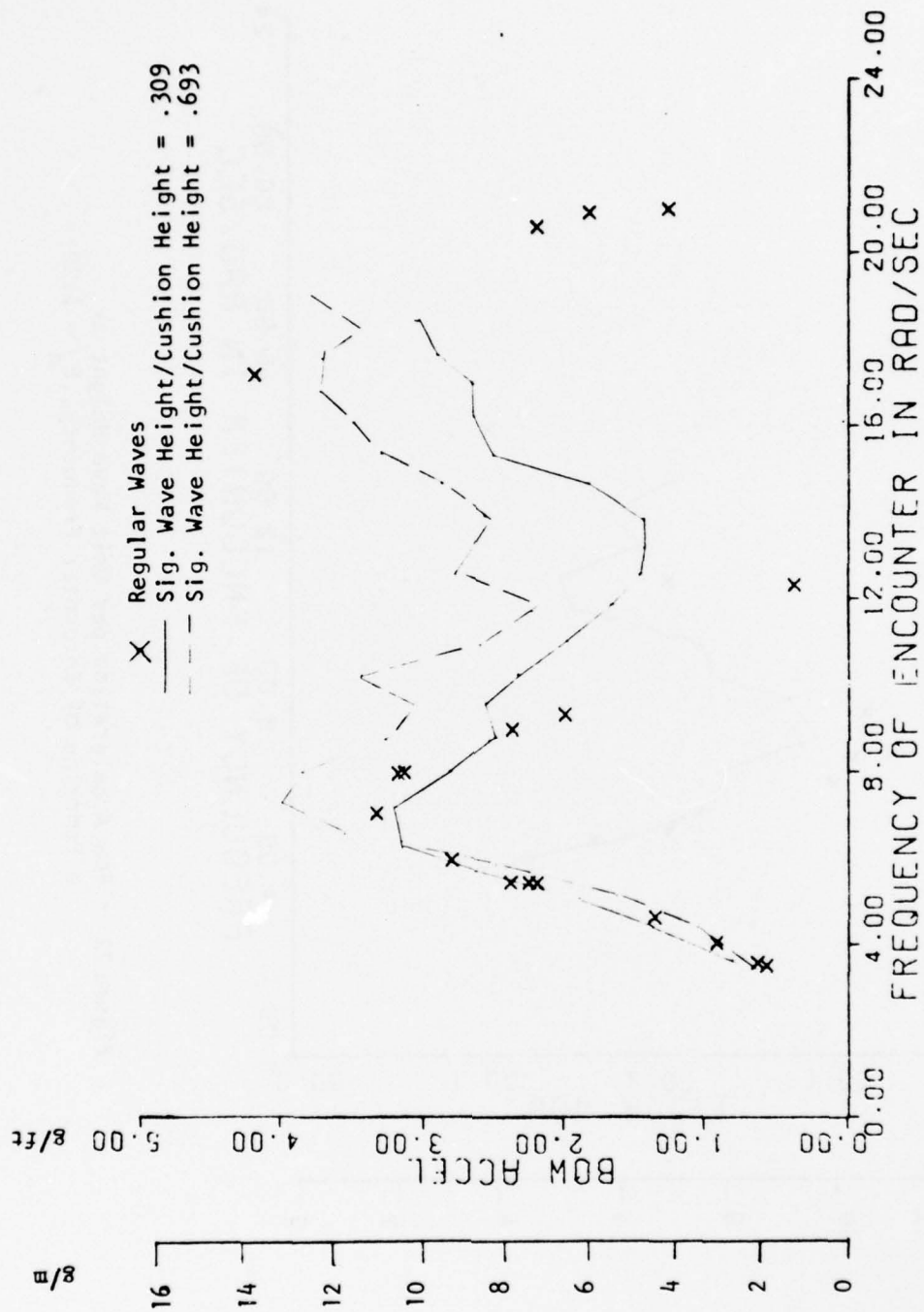


Figure 21 - Bow Acceleration per Unit Wave Height as a Function of Encounter Frequency,  $F_n = 0.96$

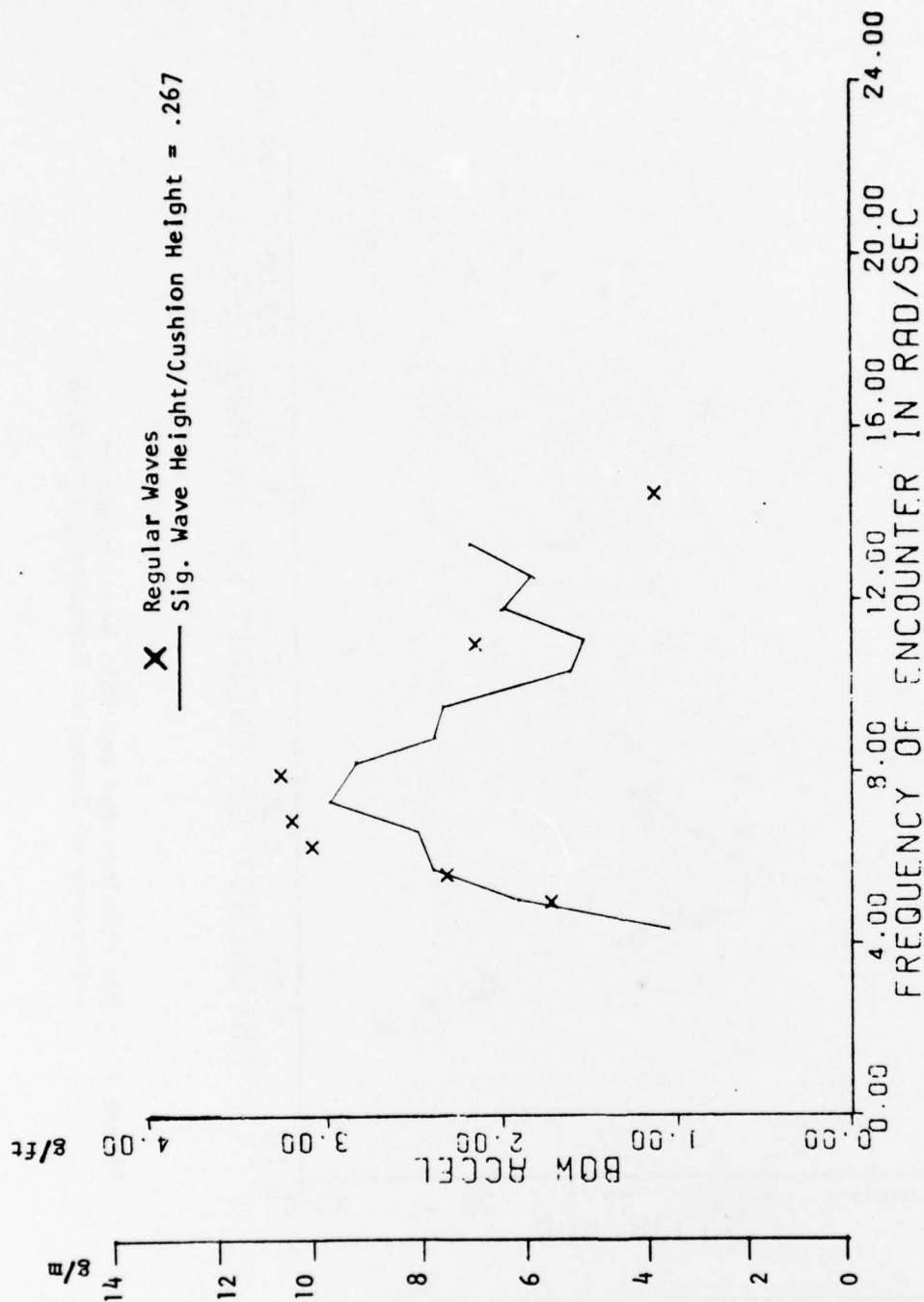


Figure 22 - Bow Acceleration per Unit Wave Height as  
 a Function of Encounter Frequency,  $F_n = 1.20$

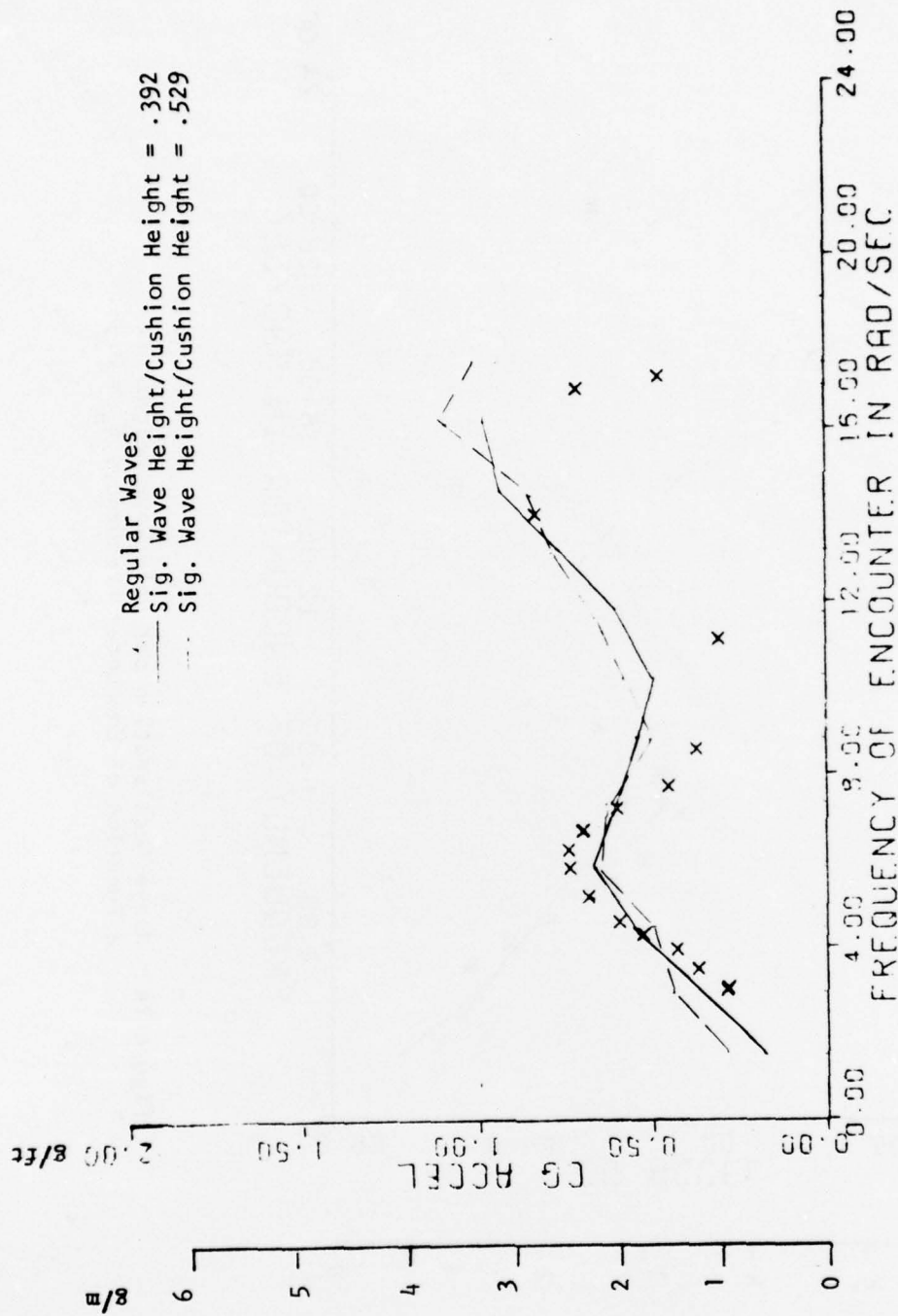


Figure 23 - Heave Acceleration per Unit Wave Height as a Function of Encounter Frequency,  $F_n = 0.72$



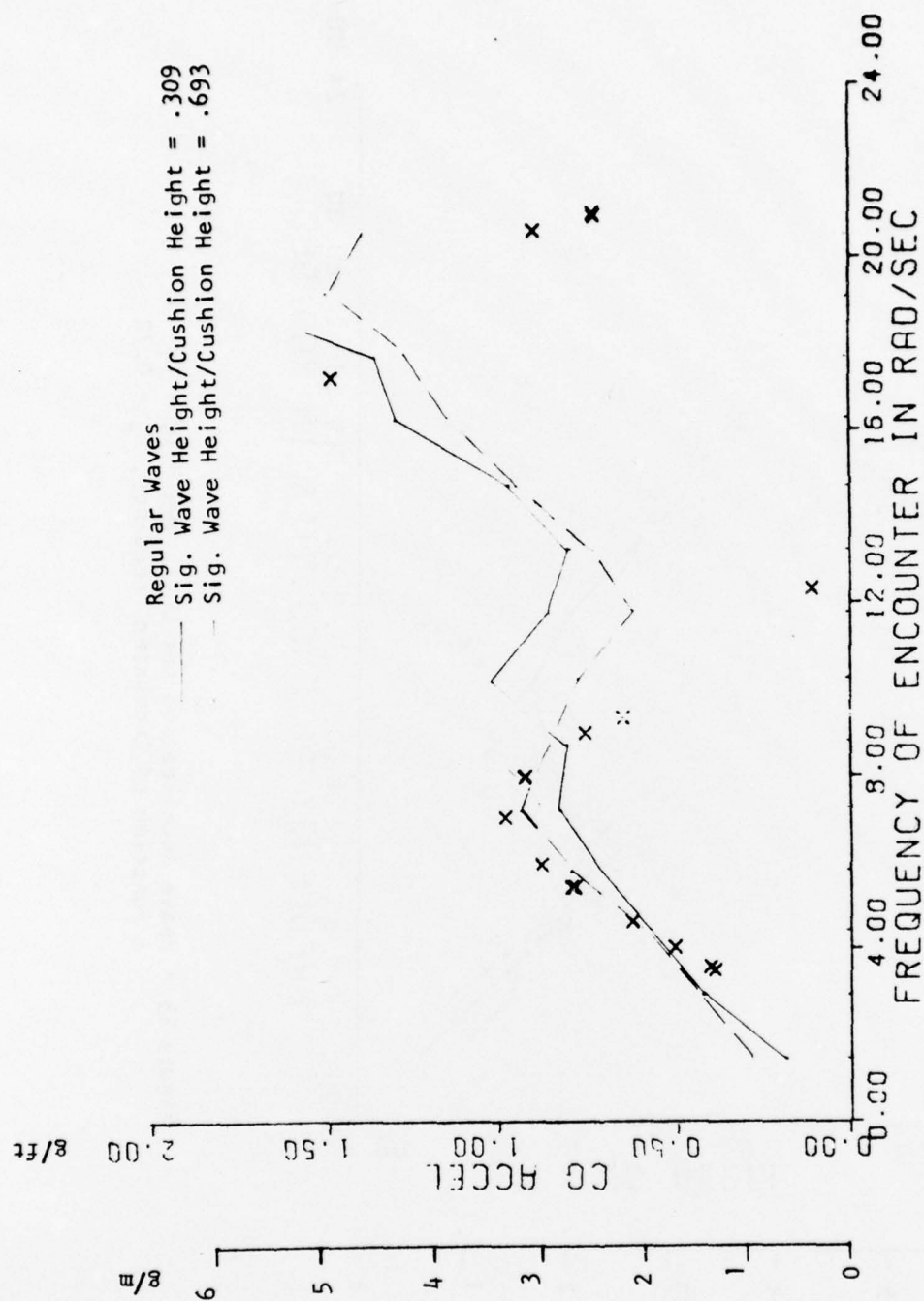


Figure 24 - Heave Acceleration per Unit Wave Height as a Function of Encounter Frequency,  $F_n = 0.96$

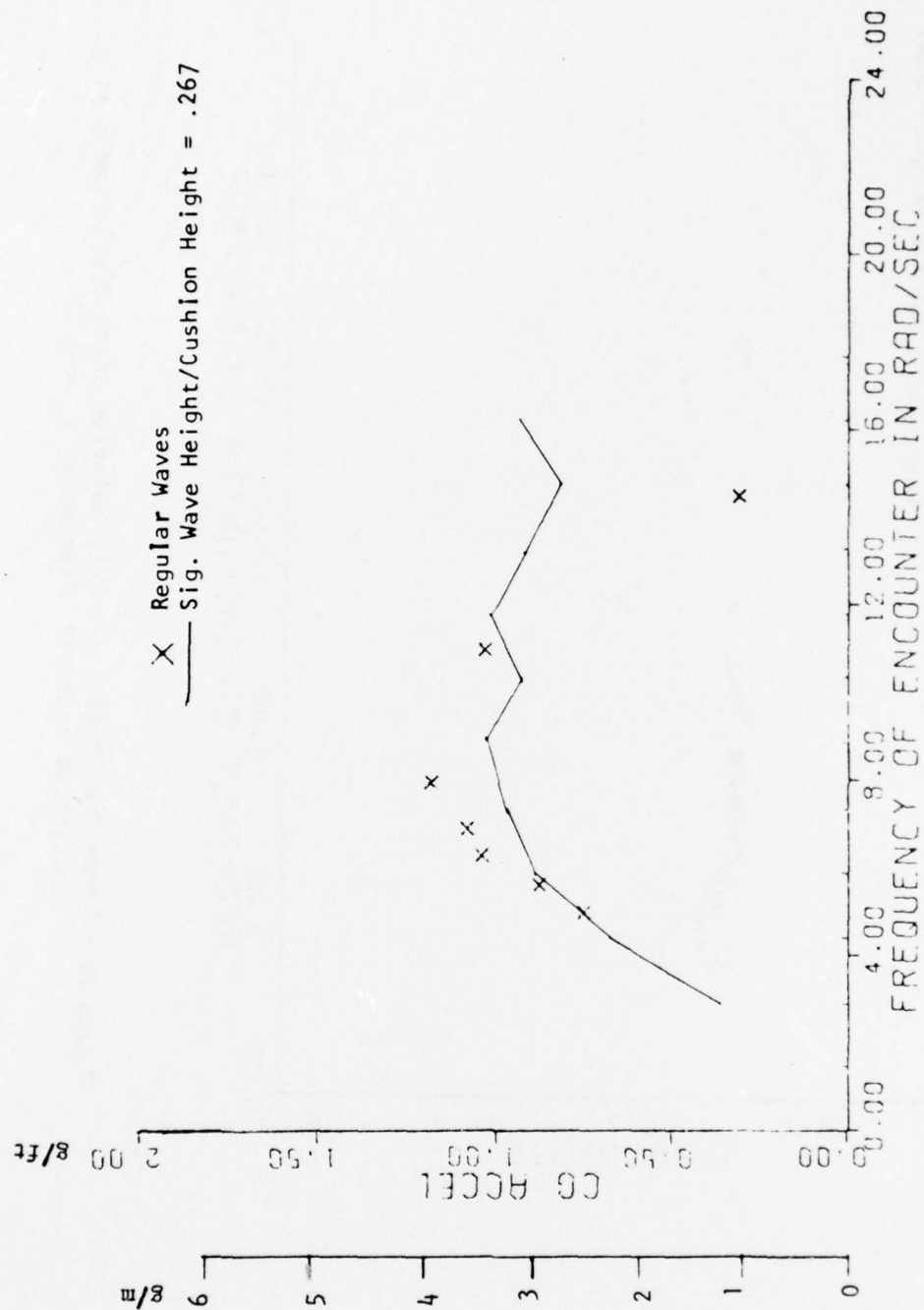


Figure 25 - Heave Acceleration per Unit Wave Height as  
 a Function of Encounter Frequency,  $F_n = 1.20$

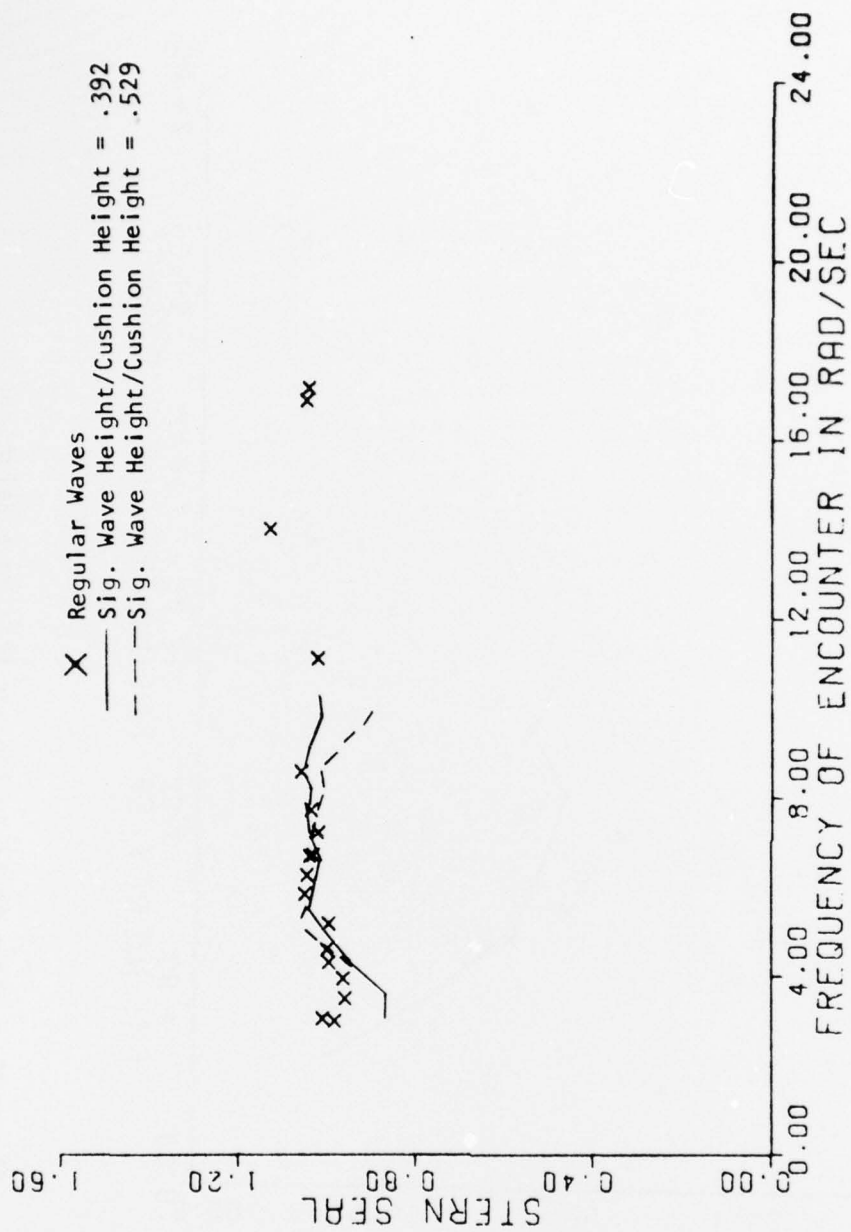


Figure 26 - Stern Seal Motion per Unit Relative Stern Displacement as a Function of Encounter Frequency,  $F_n = 0.72$

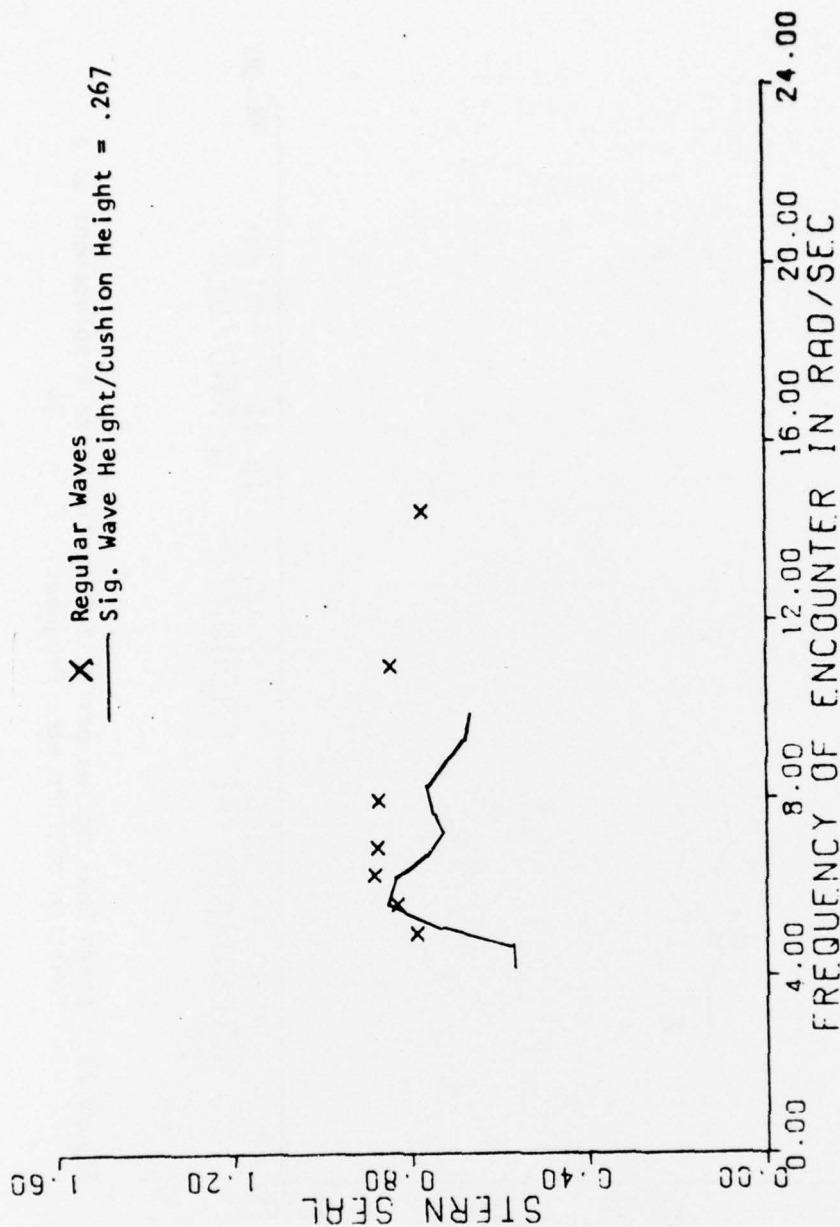


Figure 28 - Stern Seal Motion per Unit Relative Stern Displacement as a Function of Encounter Frequency,  $F_n = 1.20$

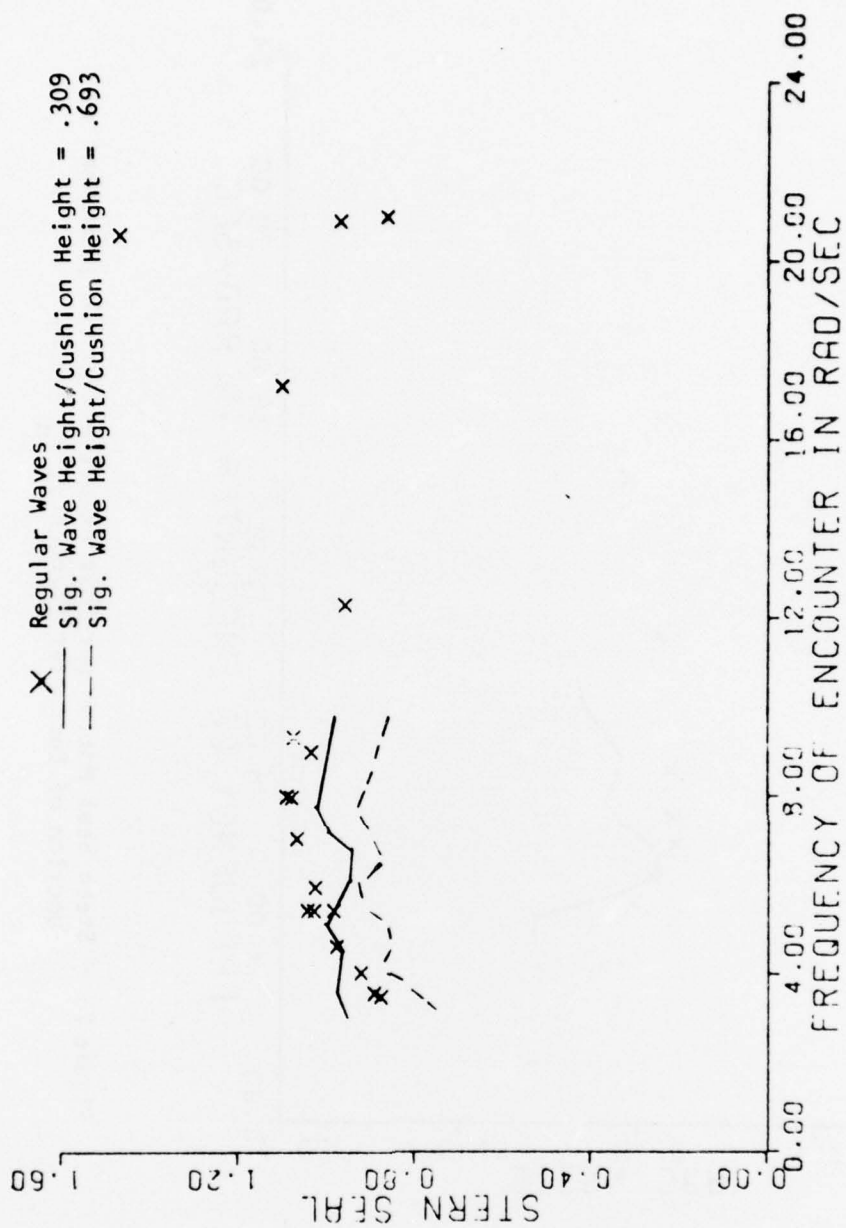


Figure 27 - Stern Seal Motion per Unit Relative Stern Displacement as a Function of Encounter Frequency,  $F_n = 0.96$



XR-5 MODEL  
 9 Knots, Head Seas  
 SIGNIFICANT WAVE HEIGHT/CUSHION HEIGHT = .392  
 ——— SAMPLE VARIANCE, --- MINIMUM  $\chi^2$  ESTIMATOR

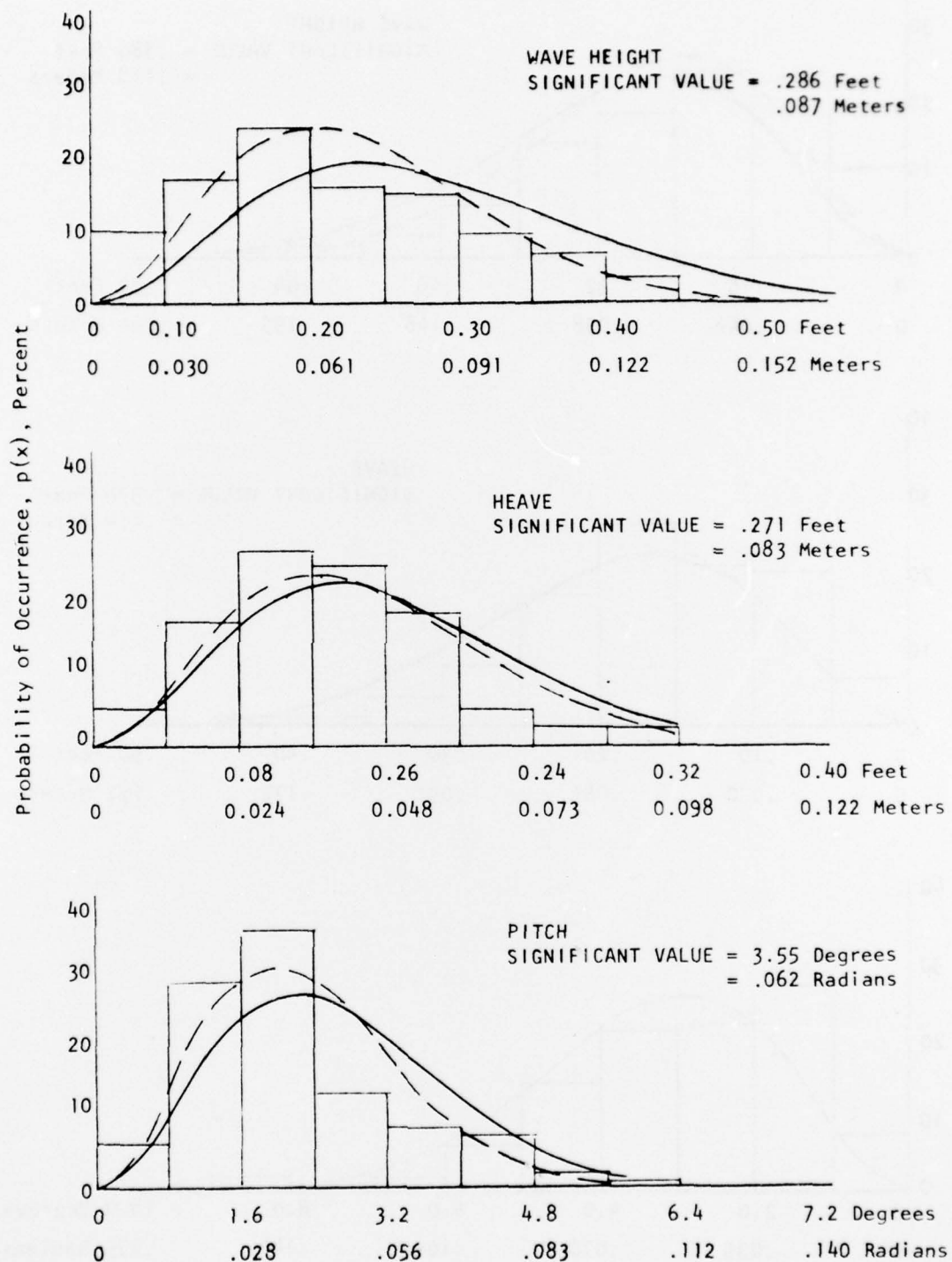


Figure 20. Double Amplitude Distributions for Heave and Pitch of the XR-5 Model at 9 Knots in Head Seas

XR-5 MODEL  
 9 Knots, Head Seas  
 SIGNIFICANT WAVE HEIGHT/CUSHION LENGTH<sub>2</sub> = .529  
 — SAMPLE VARIANCE, --- MINIMUM  $\chi^2$  ESTIMATOR

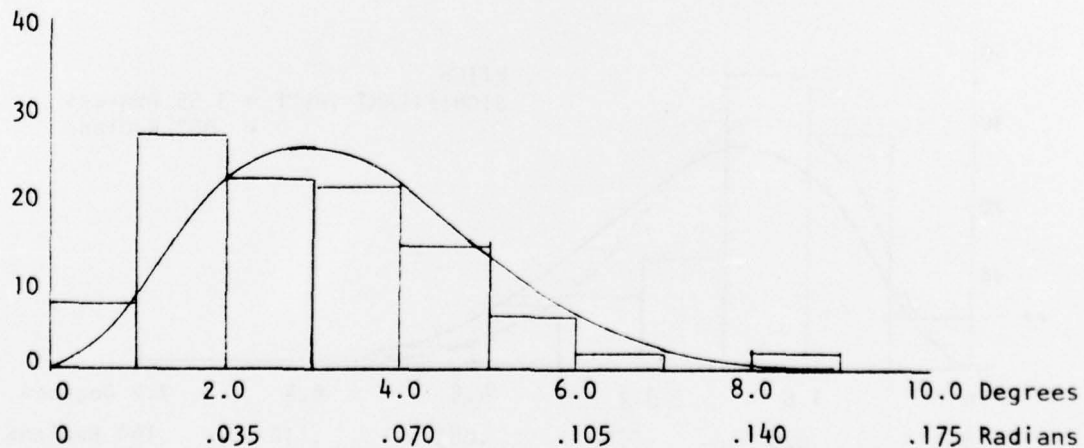
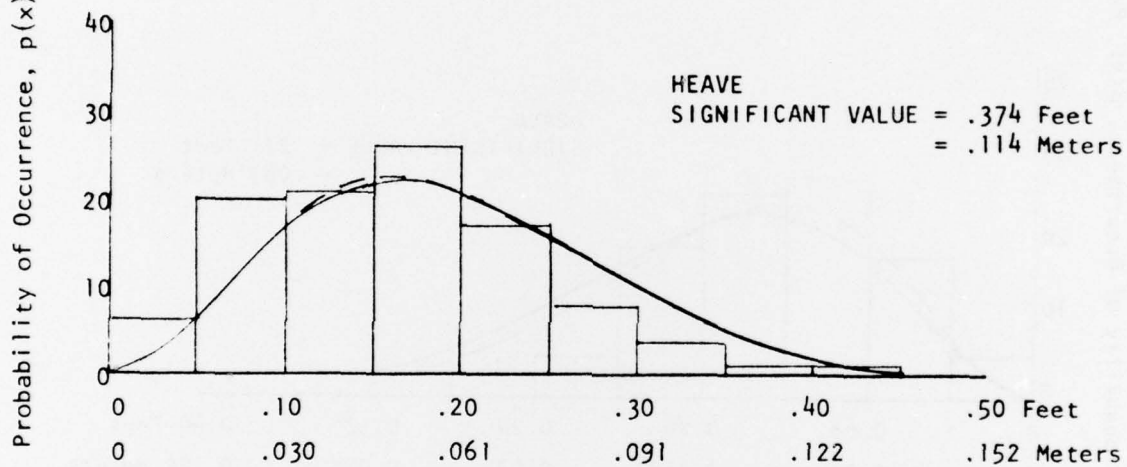
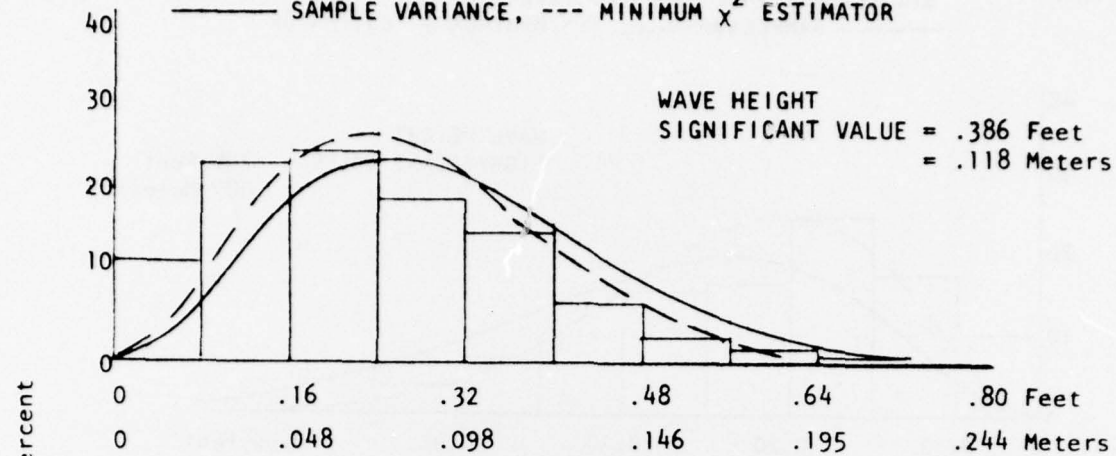


Figure 30 : Double Amplitude Distributions for Heave and Pitch of the XR-5 Model at 9 Knots in Head Seas

XR-5 MODEL  
 12 Knots, Head Seas  
 SIGNIFICANT WAVE HEIGHT/CUSHION HEIGHT = .309  
 — SAMPLE VARIANCE, --- MINIMUM  $\chi^2$  ESTIMATOR

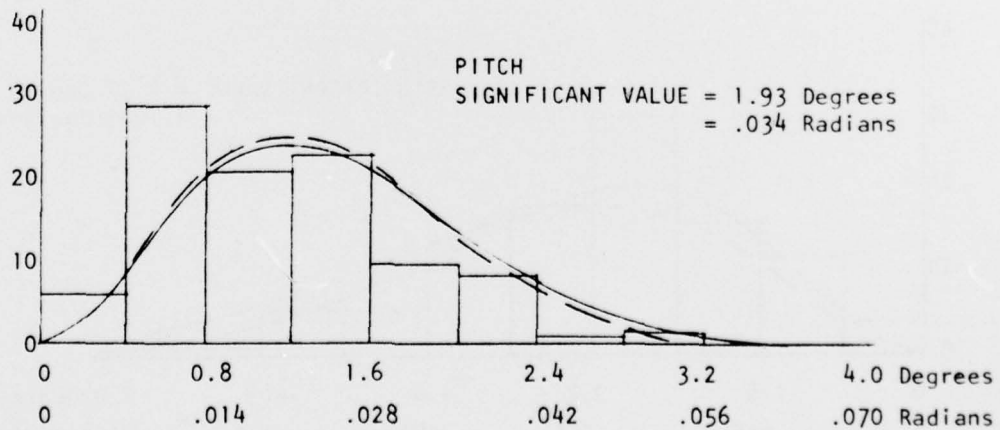
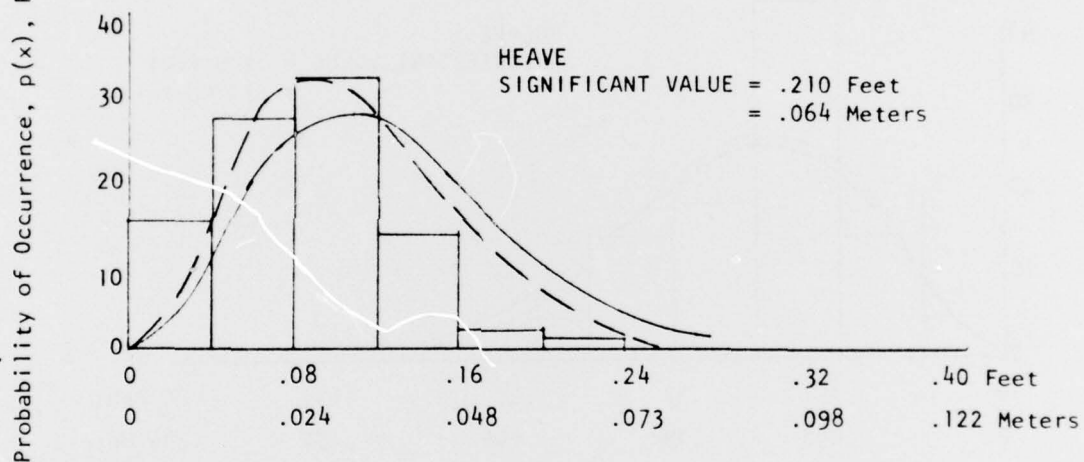
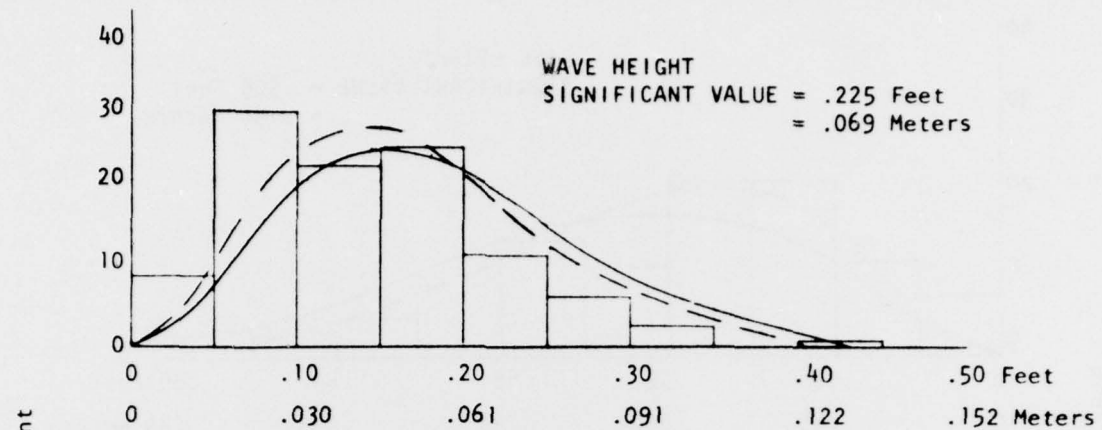


Figure 31 : Double Amplitude Distributions for Heave and Pitch of the XR-5 Model at 12 Knots in Head Seas

XR-5 MODEL  
 12 Knots, Head Seas  
 SIGNIFICANT WAVE HEIGHT/CUSHION HEIGHT = .693  
 — SAMPLE VARIANCE, --- MINIMUM  $\chi^2$  ESTIMATOR

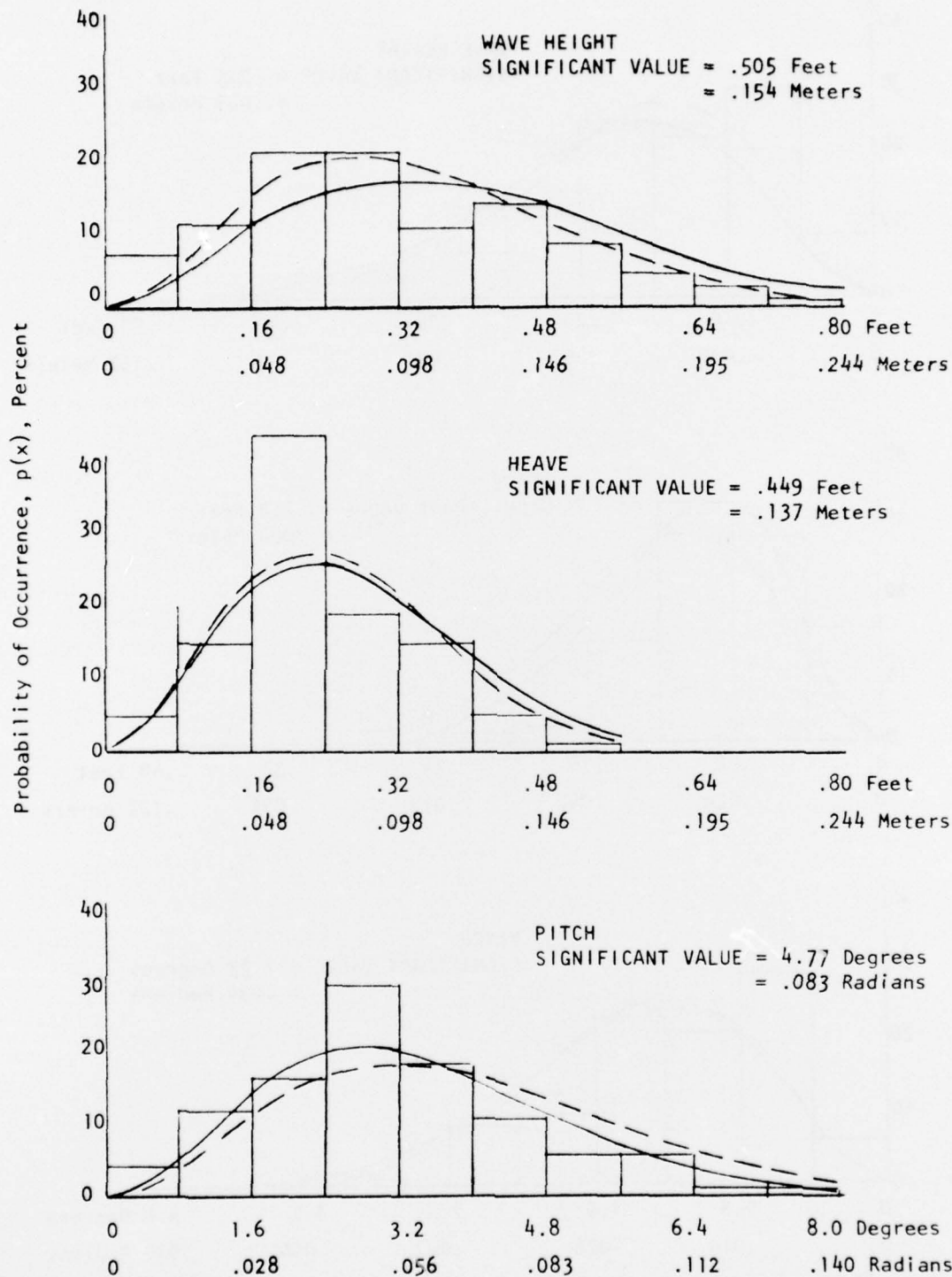


Figure 32 : Double Amplitude Distributions for Heave and Pitch of the XR-5 Model at 12 Knots in Head Seas



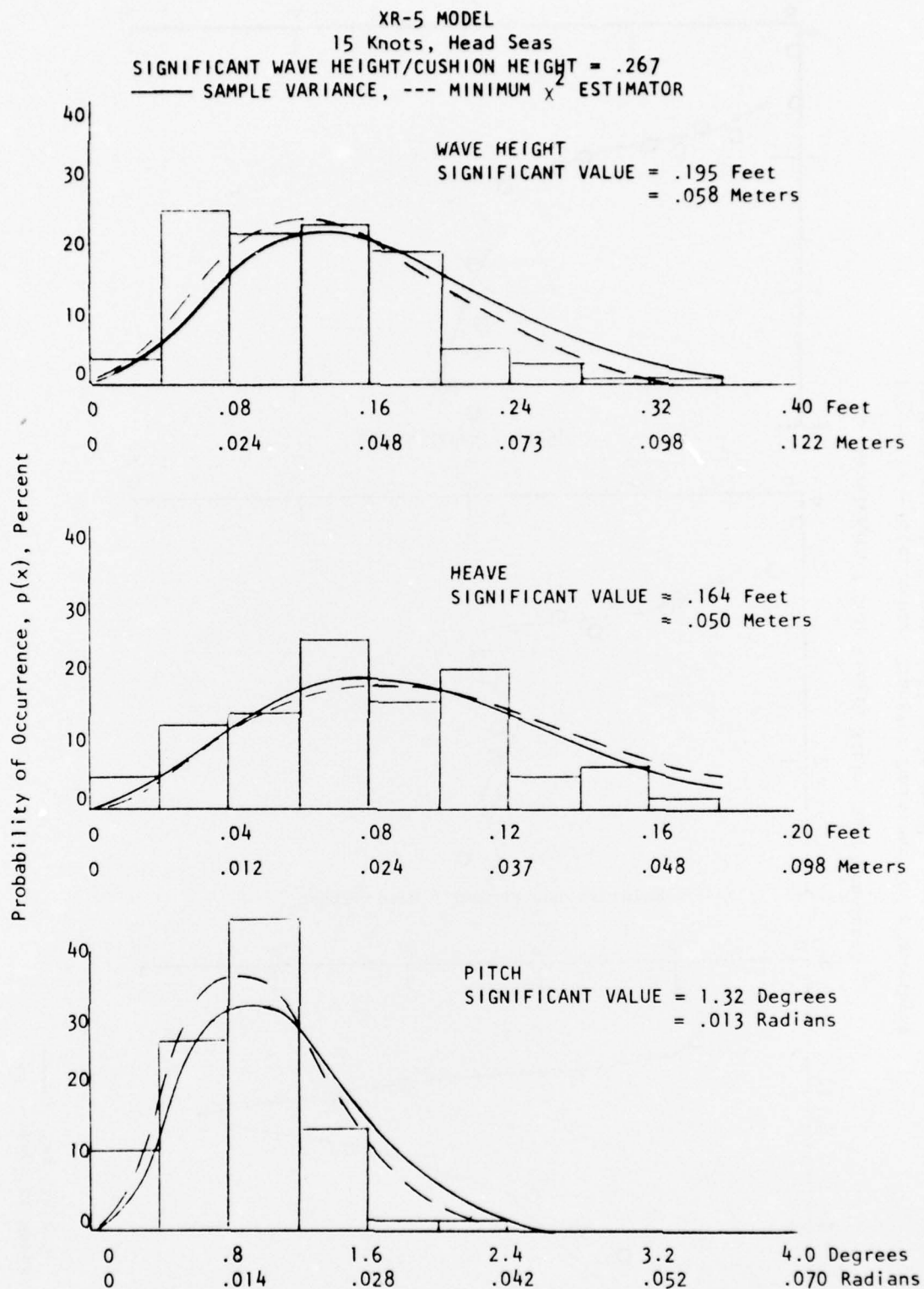


Figure 33 : Double Amplitude Distributions for Heave and Pitch of the XR-5 Model at 15 Knots in Head Seas



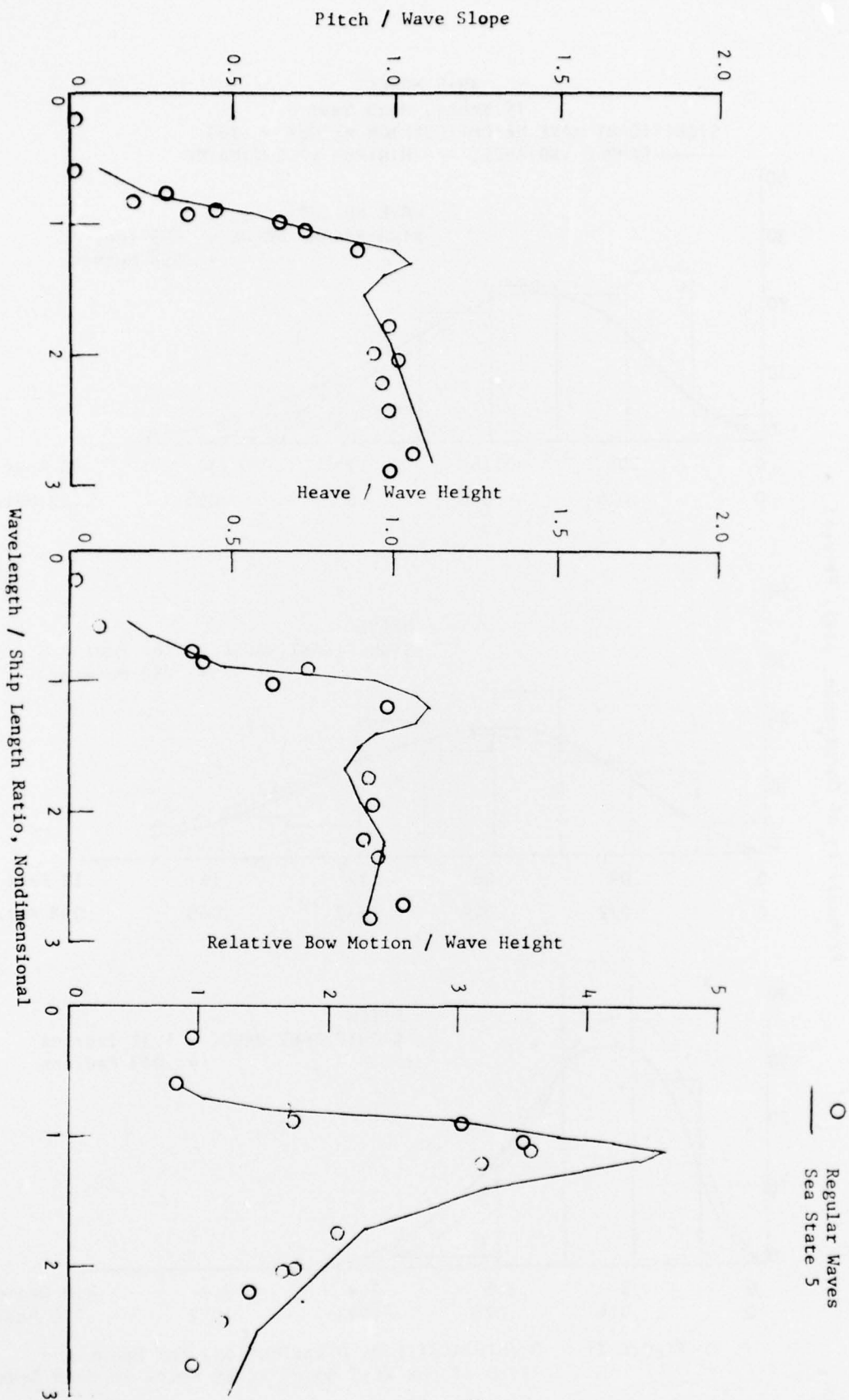


Figure 34 - Experimental Transfer Functions for a Destroyer in Head Seas at 20 Knots full scale speed

DTNSRDC ISSUES THREE TYPES OF REPORTS

(1) DTNSRDC REPORTS, A FORMAL SERIES PUBLISHING INFORMATION OF PERMANENT TECHNICAL VALUE, DESIGNATED BY A SERIAL REPORT NUMBER.

(2) DEPARTMENTAL REPORTS, A SEMIFORMAL SERIES, RECORDING INFORMATION OF A PRELIMINARY OR TEMPORARY NATURE, OR OF LIMITED INTEREST OR SIGNIFICANCE, CARRYING A DEPARTMENTAL ALPHANUMERIC IDENTIFICATION.

(3) TECHNICAL MEMORANDA, AN INFORMAL SERIES, USUALLY INTERNAL WORKING PAPERS OR DIRECT REPORTS TO SPONSORS, NUMBERED AS TM SERIES REPORTS; NOT FOR GENERAL DISTRIBUTION.